CHAPTER 4

SYNTHESIS AND CHARACTERIZATION OF BENZOCHALCOGENDIAZOLE BASED FLUORESCENT ORGANIC MOLECULES USING POLYANILINE SUPPORTED PALLADIUM

Contents

4.1 Introduction

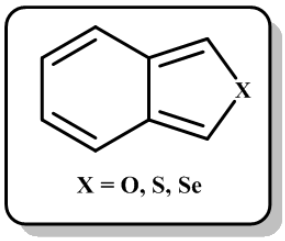

The class of heterocycles, of benzochalcogenadiazoles include benzooxadiazole (BDO), benzothiadiazole (BDT), and benzoselenadiazole (BDS). Havinga *et al.* in 1992 introduce the donor-acceptor (D-A) concept which has been extensively used to design low-band gap conjugated polymers.[1]

There is growing interest in the synthesis of small conjugated molecules compared to the polymers, due to its advantages like their easy synthesis, well-defined molecular structures, easy purification methods, better processability, ease to tune the electronic property and reproducibility. These π-conjugated systems comprising D-A-D type small molecules containing benzooxadiazole, benzothiadiazole, and benzoselenadiazole as acceptors were used in many organic electronic devices.[2] These units have also received considerable attention for applications in organic electronic such as organic field transistors (OFETs), organic light emitting diodes (OLEDs) and organic photovoltaics (OPVs).[3]

Kose *et al.* reported the star-shaped molecules (SSMs) with benzothiadiazole and benzooxadiazole groups situated in their arms as shown in Figure 1, which were used in organic photovoltaic devices. As a core moiety, benzene and silicon atoms were subjugated to yield three-arm and four-arm SSMs, respectively. The band gaps of these molecules vary between 1.83 and 2.05 eV out of which benzooxadiazole containing structures display the lower band gap signifying benzooxadiazole as a stronger electron-withdrawing group than benzothiadiazole.[4]

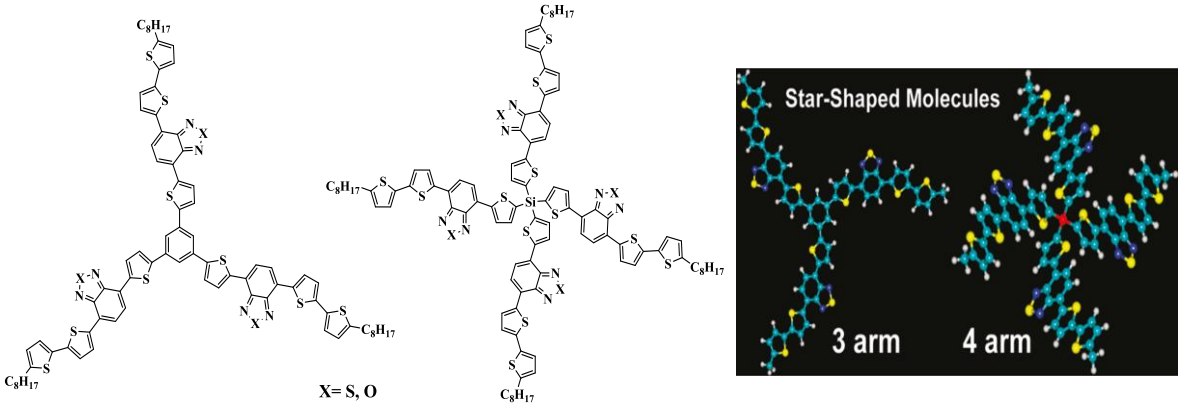

Figure 1: Low band gap star-shaped molecules based on benzothia(oxa)diazole

Zade *et al.* synthesized series of D-A-D type small molecules comprising of benzooxadiazole (BDO) and benzothiadiazole (BDT) core symmetrically linked to two aromatic-heterols as shown in Figure 2 which showed good application in field effect transistor. Due its easy solubility in common solvents and good thermal stability, these molecules can be used for flexible electronics. In this report devices based on the solution processable all organic field effect transistors demonstrated hole mobility as high as 0.08 cm^2V^{-1} s^{-1} and I_{on}/I_{off} ratio of 10^4.[5]

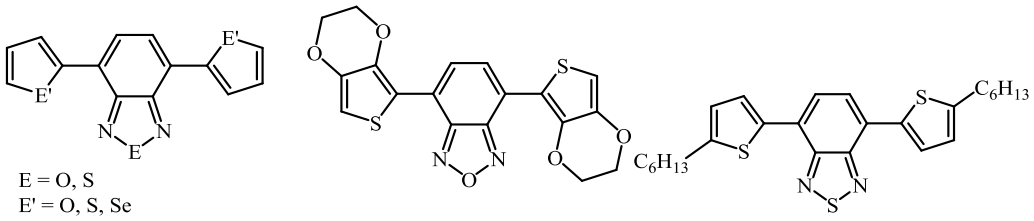

Figure 2: Benzooxadiazole and benzothiadiazole based D-A-D Molecules

Bunz *et al.* synthesized water-soluble highly fluorescent bis-triazolyl benzochalcogendiazole cycloadducts and reported as tuneable metal ion sensors as shown in Figure 3. The cycloaddition of an ethynylated benzochalcogendiazole and a water-soluble azide gave the corresponding florophores. These compounds reveals a lowering of the band gap on going from oxygen to selenium, as well as an increase in the binding efficiency of copper and nickel ions.[6]

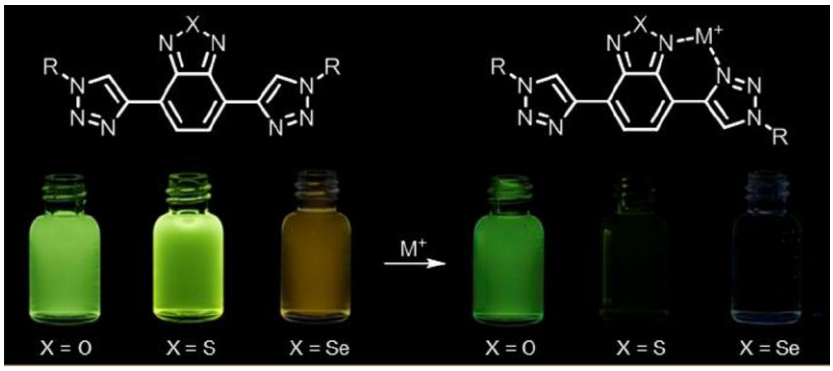

Figure 3: Bis-triazolyl benzochalcogendiazole cycloadducts as metal ion sensors

Shinoda *et al.* reported benzothiadiazole-based dyes that emit red light in solution, solid and liquid state as shown in Figure 4. They observed an efficient red light emission with high fluorescence quantum yields (up to 0.78) and with increase in solvent polarity, the

emission bands shifted to longer wavelengths accompanied by a large Stokes shift of up to 152 nm.[7]

Figure 4: BDT based dyes and florescence images in solution, solid and liquid

Justin Thomas *et al.* synthesized benzothiadiazole-based organic dyes containing pyridine anchoring group and different for nitrogen-based heterocyclic electron donating units linked via benzothiadiazole moiety as shown in Figure 5 and did its application as dye-sensitized solar cells. The dye-sensitized solar cells fabricated using a dye containing phenothiazine donor showed power conversion efficiency of 1.97%.[8]

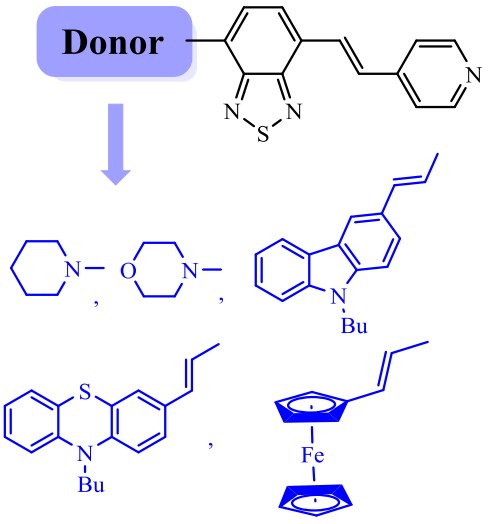

Figure 5: Structures of pyridine anchoring sensitizers featured with BTD

By making small changes in the molecular architecture conjugated molecules notably changes its electrochemical and optical properties.[9] Therefore, small conjugated molecules have been synthesized and their structure-property correlation have been studied.

Organic transformations mediated by heterogeneous metal catalysts, particularly prepared with costly and toxic metal ions, is a useful option in modern organic chemistry. In our earlier

chapter, we have discussed the importance of PANI as a solid support for palladium and also explore it as a heterogeneous catalyst for various organic transformations. Looking at the importance of benzochalcogenadiazoles based conjugated molecules we have used our catalytic system for the synthesis of a new class of benzochalcogenadiazoles by C-C coupling reactions.

4.2 Results and discussion

In this chapter we present application of Polyaniline loaded Palladium catalyst for synthesis of small molecules by Suzuki-Miyaura reaction & Mizoroki-Heck reaction. Furthermore using this catalyst system we have prepared various benzothiadiazole based conjugated organic molecules by one pot Wittig-Heck reactions to study the effect of R group on donor part of fluoroscent molecules.

4.2.1 Synthesis of benzochalcogendiazole based fluorescent organic molecules by Suzuki and Heck reaction using PANI-Pd

4.2.1.1 Synthesis of dibrormobenzochalcogendiazoles

Synthesis of all the three dibromo benzochalcogendiazoles were done by reported procedure as shown in scheme 1. In the first step we synthesized 4,7-dibromo-2,1,3-benzooxadiazole **5**, starting with 2-nitroaniline by oxidatively cyclized to benzofuroxan **2** with commercial bleach, and then deoxygenated to benzofurazan 2,1,3-benzooxadiazole, **3** with triethyl phosphate and purified by vacuum sublimation. Bromination with molecular bromine in hydrobromic acid affords the tetrabromo compound **4** which is further treated with 1,8-diazabicyclo[5.4.0]undec-7-ene (DBU) in tetrahydrofuran at room temperature to yield compound **5**.[10] For the synthesis to 4,7-dibromo 2,1,3-benzothiadizole **8,** *ortho*-phenylene diamine **6** was treated with thionyl chloride to achieve benzthiadiazole **7**, which on further treated Br_2 in HBr gives **8**. Further compound **8** is reduced by lithium aluminium hydride yield 3,6-dibromobenzene-1,2-diamine **9** which on reaction with selenium dioxide gives 4,7-dibromo 2,1,3-benzoselenodizole **10.**[11]

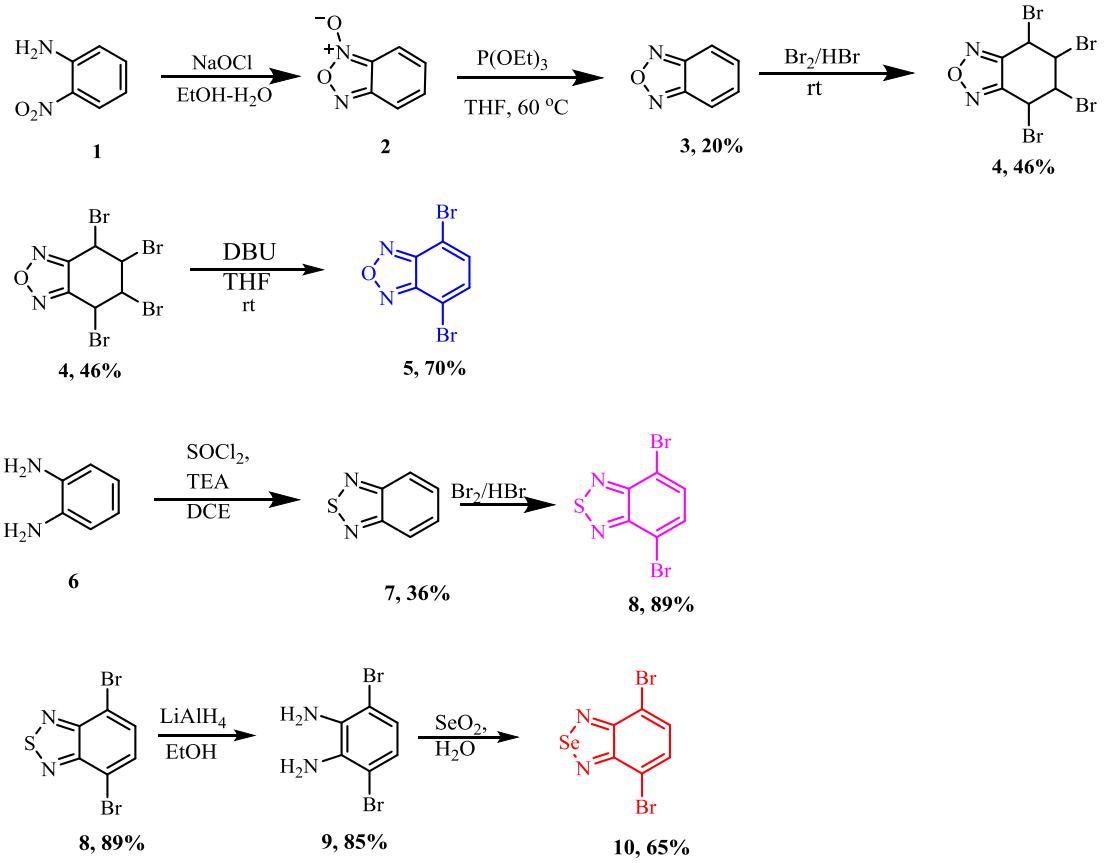

Scheme 1: Synthesis of di bromo benzo oxa/thia/seleno diazole

4.2.1.2 Application of polyaniline supported palladium for Suzuki Miyaura and Mizoroki-Heck reaction

The catalyst system was then applied for Suzuki-Miyaura coupling reaction. The standard reaction condition is shown in Scheme 2, where dibromo benzochalcogendiazole was treated with phenyl/thiophene boronic acid in the presence of PANI-Pd catalyst and the suitable base. The biaryls, product of this coupling reaction, were isolated in high yields and characterized by the usual spectroscopic techniques.

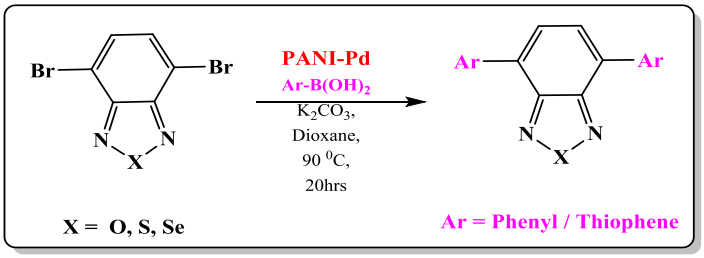

Scheme 2: PANI-Pd catalyzed Suzuki-Miyaura reaction

A series of molecules were subjected to the above Suzuki-Miyaura condition with phenyl boronic acid for **11-13**, with thiophene boronic acid for **14-16** and all the products were isolated in good yields (Scheme 3).

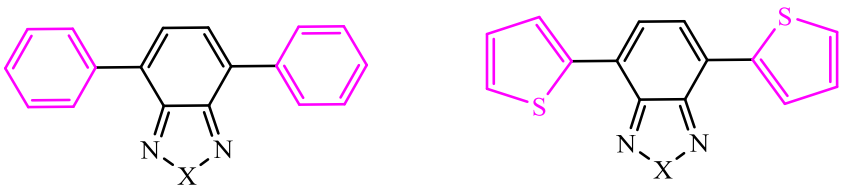

11, X = O (87%)
12, X = S (83%)
13, X = Se (81%)

14, X = O (78%)
15, X = S (80%)
16, X = Se (70%)

Scheme 3: Molecules prepared by Suzuki-Miyaura reaction with PANI-Pd catalyst

The synthesized PANI-Pd catalyst was then examined for the standard Mizoroki-Heck coupling reaction of Further, dibromo benzochalcogendiazole were subjected Mizoroki-Heck coupling reaction with different styrene derivatives in presence of a PANI-Pd and mild base, K_2CO_3. (Scheme 4)

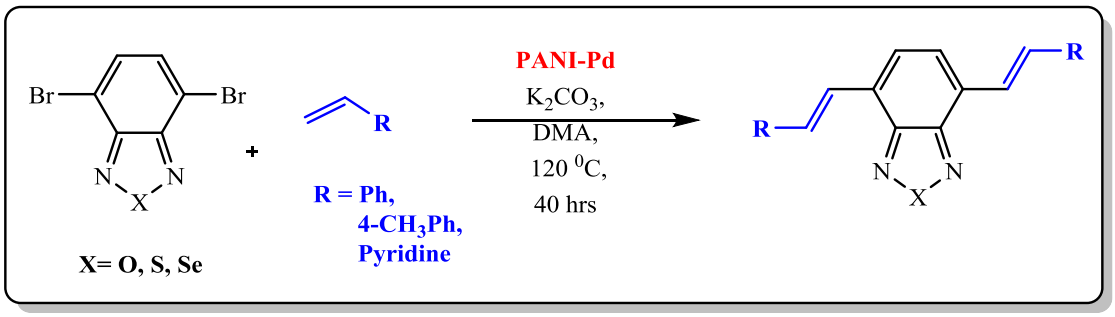

Scheme 4: PANI-Pd catalyzed Mizoroki-Heck reaction

Under the above conditions for the Mizoroki–Heck reaction, the stilbene derivatives are obtained in good yields, and isolated mostly as the *E*-isomer as shown in scheme 5. All the synthesized stillbene derivatives were characterized by the usual spectroscopic techniques.

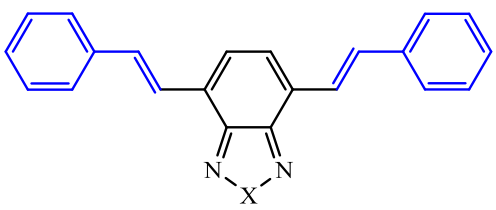

17, X= O (74%)
18, X= S (71%)
19, X= Se (69%)

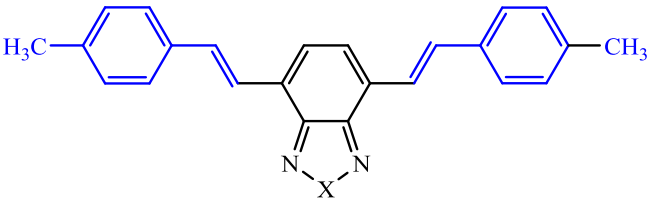

20, X= O (72%)
21, X= S (73%)
22, X= Se (65%)

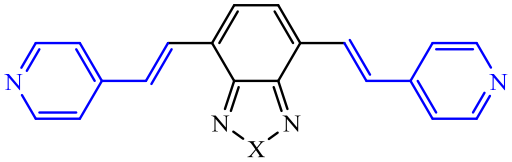

23, X= S (31%)
24, X= Se (26%)

Scheme 5: Molecules prepared by Mizoroki-Heck reaction with PANI-Pd catalyst

4.2.1.3 Photophyscial studies

All the synthesized derivatives were highly florescent in solid state as well as in diluted solution. Figure 6 shows photograph taken under (365 nm) UV lamp in chloroform solution.

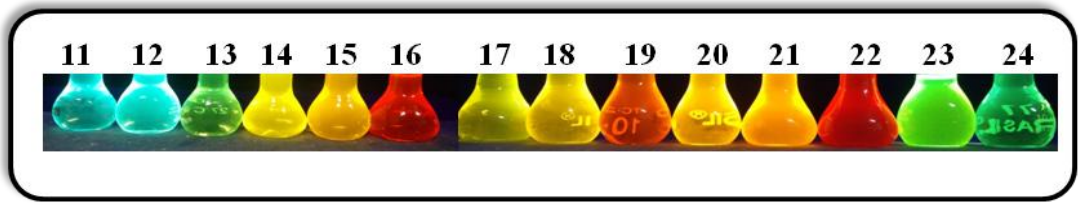

Figure 6: Compounds **11** to **24** as viewed under UV light in solution

The absorption and emission spectra of all the synthesized compounds were studied in chloroform solution with concentration of 10^{-5} M. Absorption spectra of compounds **11-16** shows bands between 370-550 which are assigned to charge transfer transitions (CT, D-A) (Figure 7). The absorption spectrum of compounds **14-16** are red-shifted compared to compounds **11-13** as there is increase in electron donation capacity of thiophene ring compared to normal phenyl ring. Emission spectra of compounds **11-16** exhibit emission maxima between 484-620 nm with stoke shift between 102-140 nm as shown in Table 1. Compound **11** shows blue shift with emission maxima at 484 nm, whereas compound **16** shows emission maxima 620 nm, exhibiting a red shift of 136 nm.

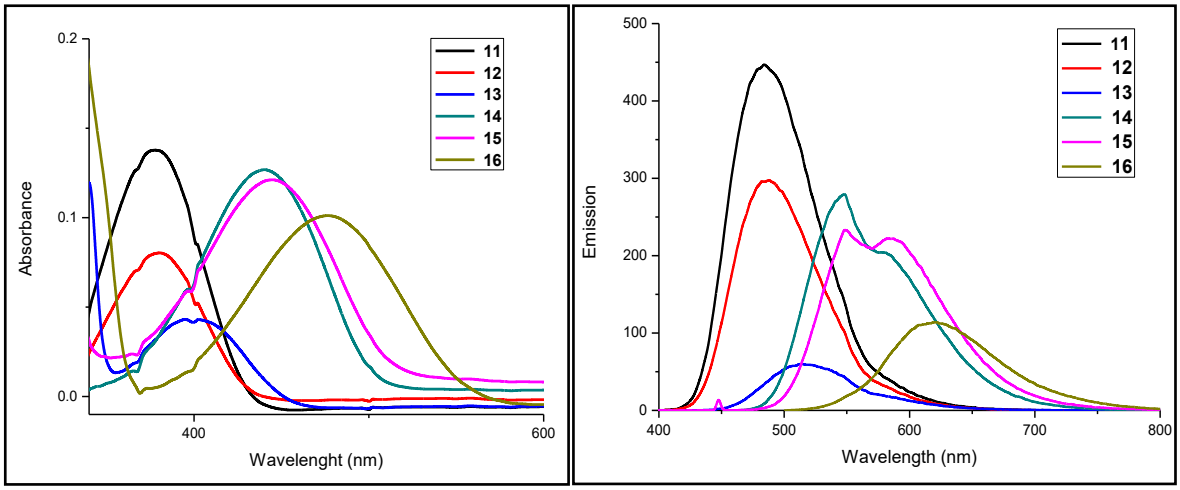

Figure 7: Absorption Spectra (left) and Emission Spectra (right) of Molecules prepared by Suzuki-Miyaura reaction

The absorption spectra of the compounds **17-24** having additional double bond synthesized by Heck reaction were studied. It is established that these molecules can have *cis-cis*, *cis-trans* and *trans-trans* forms contributing to distinctly different optical and physical properties.[12] But we have determined that all molecules have *trans-trans* configuration, which is established by ^{1}H-NMR analysis. It possesses a characteristic dual band nature, the higher energy band (250-350 nm) are due to $\pi \rightarrow \pi^*$ transition of the conjugated backbone and lower energy band are due to $n \rightarrow \pi^*$ or by charge transfer. Like in the earlier case the absorption spectrum of compounds **20-22** are slightly red-shifted compared to compounds **17-19** due to addition of methyl group which is donating group. As pyridine is a π-deficient heterocyclic ring with electron accepting character it exhibits lower emission maxima 427 and 456 nm (compound **23** and **24**) compared to compound **18** and **19** which shows 450 and 451 nm respectively. Further, spectral examination indicates that the λ_{em} for compounds **17-24** varied in the range of 103 nm, that is, from 521 nm for compound **23** to 624 nm for compound **22** as shown in Figure 8 and Table 1.

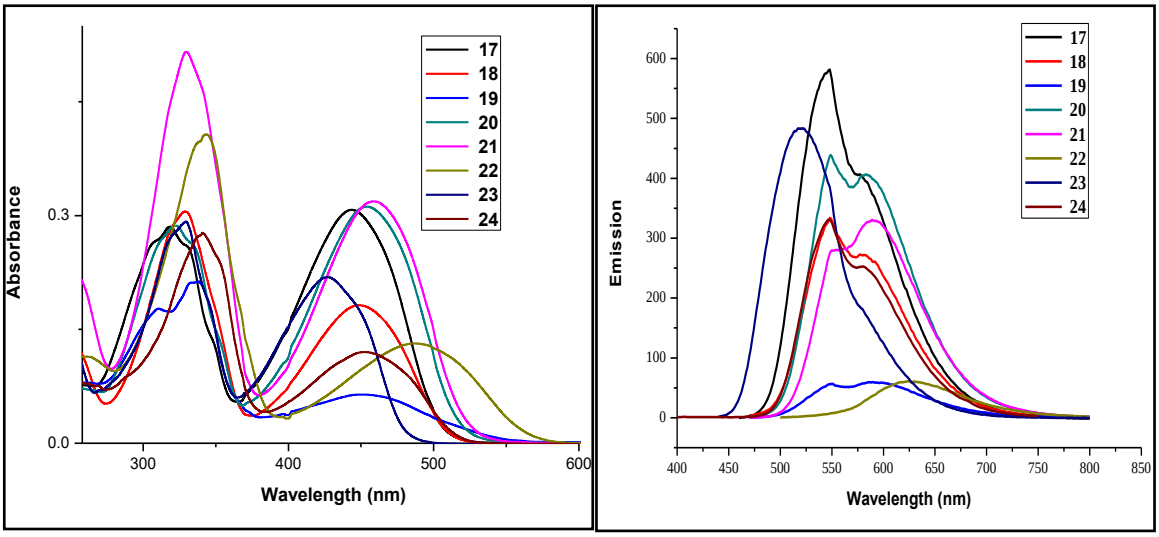

Figure 8: Absorption and Emission Spectra of Molecules prepared by Heck reaction

Comparison of the absorption spectra of compound **11-13** and **17-19**, shows that by inserting a double bond between benzochalcogen moiety and phenyl group a visible change in red shift from 377-390 nm (for compound **11-13**) to 444-451 nm (for compound **17-19**) is observed. This is due to increase in electron donation capacity which resulted in to decrease in optical band gap as shown in Table 1.

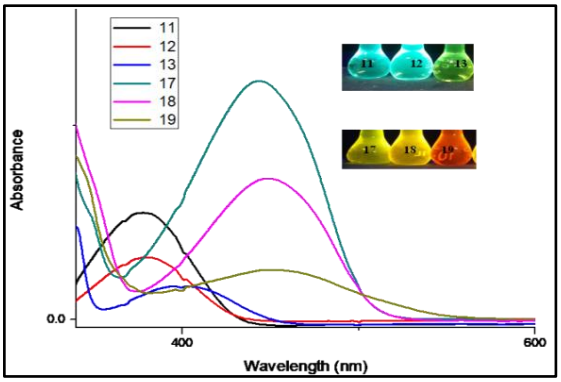

Figure 9: Absorbance spectra of compounds **11-13** and **17-19**

General observation we have obtained in both the cases is λ_{max} values of peak exhibit a red shift when heavier chalcogen are substituted into the benzodiazole unit. This could be attributed to the increase in the electron density and atomic radius of the heteroatom (from O to Se) resulting in an improved intramolecular charge transfer (ICT).[13]

In the absorption spectra there is decrease in intensity of BDS-based compounds compared to BDT and BDO based compounds. This can be ascribed to decrease in

electronegativity of heteroatom from oxygen to sulphur to selenium. As oxygen has higher electronegativity compared to sulphur and selenium, BDO unit has higher ability to produce and stabilize a charge-separated state.[5,14] Moreover in emission spectra of compounds **14,15,18-21** and **24** showed vibronic progression due to distinct transitions associated with a typical C-C stretching motion strongly coupled to the electronic system suggesting the dominance of single molecule species. The absence of such vibronic features in indicates the presence of highly aggregated species in solution.[15]

Table 1: UV-vis, fluorescence and some electrochemical data for compounds 11-24

Sr.No.	Compound	λ_{max} Absorbance nm	λ_{max} Emission Nm	λonset	Stoke shift nm	ε	E_{gap}^{op} (eV)
1.	**11**	378	484	444	106	13785	2.79
2.	**12**	380	488	456	108	8038	2.72
3.	**13**	399	512	480	113	4156	2.58
4.	**14**	440	548	506	108	12682	2.45
5.	**15**	447	549	521	102	12099	2.38
6.	**16**	480	620	555	140	10073	2.23
7.	**17**	444, 319	548	506	104	30762	2.45
8.	**18**	450, 329	549	509	99	18182	2.44
9.	**19**	451, 337	585	540	134	6418	2.30
10.	**20**	453, 321	549	534	90	31171	2.32
11.	**21**	460, 329	589	540	129	31861	2.30
12.	**22**	489, 344	624	582	135	13129	2.13
13.	**23**	427, 329	521	479	100	21883	2.59
14.	**24**	456, 341	548	516	92	11957	2.40

The presence of terminal pyridine group in compound **23** was studied, as nitrogen of pyridine ring is active and can easily be protonated and hence can significantly alter the absorption and emission of compound. The pyridine terminated **c**ompound **23** was studied for its protonation behavior spectroscopically. The absorption spectrum of compound **23** showed a strong absorption in the range of 280-500 nm, where the absorption near 300 nm can be assigned to π-π* electronic transitions while the absorption band near 450 nm can be due to n-π* transition. Upon addition of dilute methanolic HCl the absorption band 329 nm almost

disappears, while band at 421 nm increases in intensity and shifts to 427 nm as shown in Figure 10.

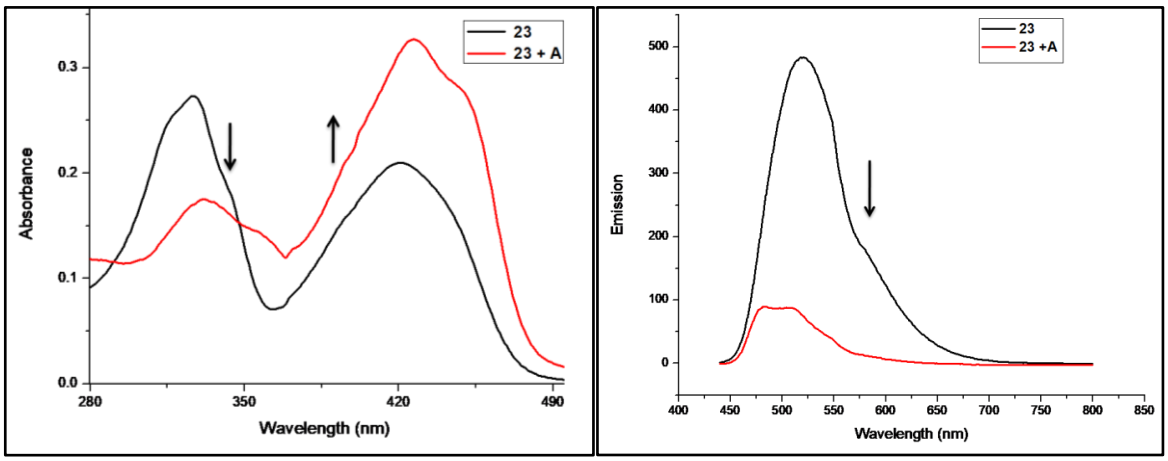

Figure 10: Absorption and Emission Spectra of compound **23** before and after addition of methanolic HCl

This compound is highly fluorescence under neutral conditions but exhibit almost no fluorescence upon addition acid as shown in Scheme 6. It was confirmed by emission spectra which shows quenching upon addition of acid. Quenching is observed in presence of HCl and by addition of ammonia it is regenerated making the process reversible which can be attributed to the protonation-deprotonation process of the terminal pyridine groups, which allows the reversible inter-conversion between the cationic and neutral forms of **23**.

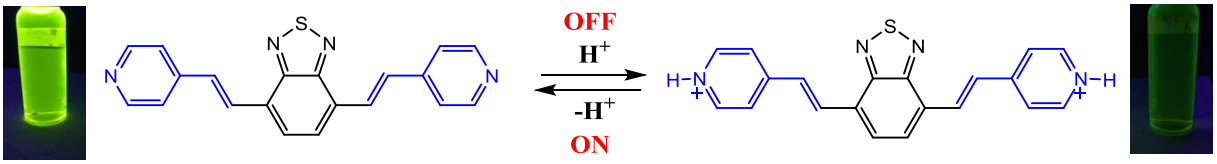

Scheme 6: Acid- responsive fluorescent compound **23**

4.2.1.4 Single crystal X-ray diffraction (SCXRD) study:

Crystals of **18, 19** and **22** were obtained by slow evaporation method from ethyl acetate-pet ether system. The molecular structures of compounds are shown in Figure 11.

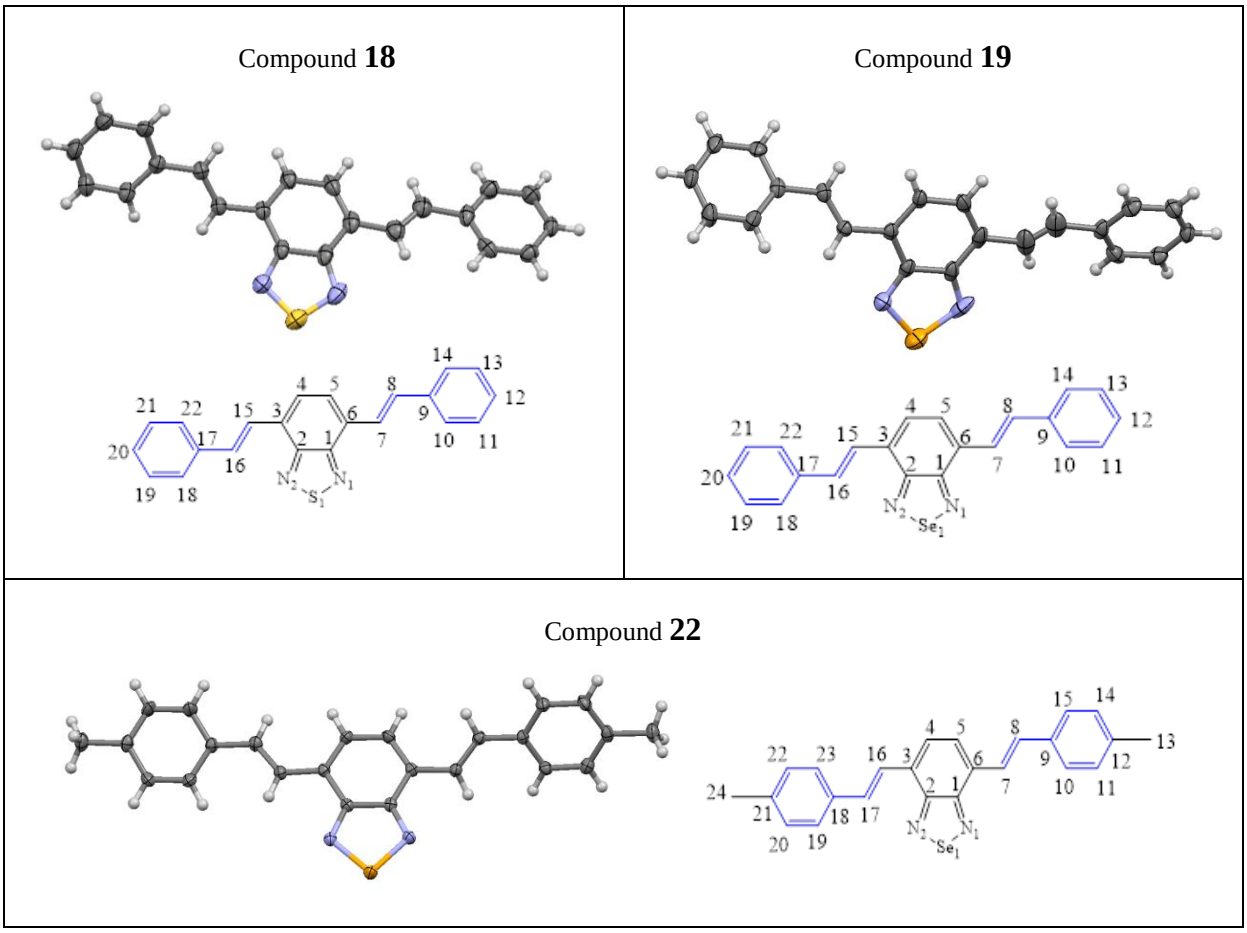

Figure 11: Molecular structures of compounds **18, 19** and **22**

Table 2: The selected bond lengths and angles of compound 18,19 and 22

	Bond Length		Bond Angles	
Compound **18**	*N1---S1*	1.613	*N1-S1-N2*	100.60
	N2---S1	1.607	*C6-C7-C8*	124.70
	C7---C8	1.336	*C9-C8-C7*	125.58
	C15---C16	1.303	*C3-C15-C16*	124.12
			C17-C16-C15	126.67
Compound **19**	*N1---Se1*	1.786	*N1-Se1-N2*	94.72
	N2---Se1	1.767	*C6-C7-C8*	122.80
	C7---C8	1.304	*C9-C8-C7*	125.54
	C15---C16	1.190	*C3-C15-C16*	120.44
			C17-C16-C15	122.89
Compound **22**	*N1---Se1*	1.778	*N1-Se1-N2*	94.31
	N2---Se1	1.780	*C6-C7-C8*	128.44

	C7---C8	1.334	*C9-C8-C7*	126.62
	C15---C16	1.338	*C3-C16-C17*	125.84
			C18-C17-C16	126.98

Compounds **18** and **19** gets crystallized into monoclinic crystal system with space group Pc (for 1) and P21/c while compound **22** get crystallized into triclinic crystal system with P-1 space group. The molecular packing of compound **18** and **19** follows similar crystal packing structure. Significantly π----π stacking was observed which might facilitate charge hopping and forms 1-D ladder like structure (Figure 12) and a 2-D interlock pattern like structure (Figure 13). Intermolecular supramolecular interactions such as π---π and CH----π favours the interlock type of packing. Due to π----π stacking and CH---π stacking, compounds get arranged anti to each other. Compound **22** forms a clockwise rotating mill like packing (Figure 14) along ac axis due to strong CH---π interaction. The both benzene rings are syn in position for all three compounds while the allylic system forms a Z configuration. The selected bond lengths and angles of the title compounds are listed in Table 2.

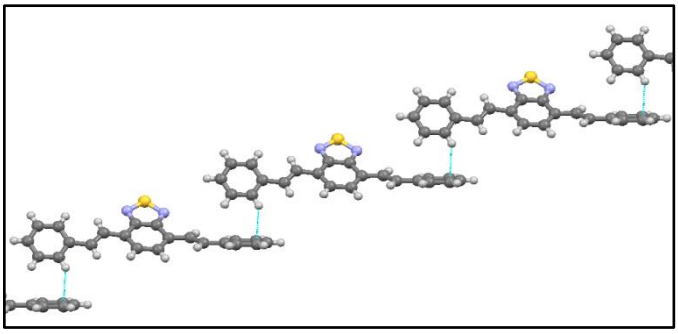

Figure 12: 1-D ladder like structure in compound **18** along b-axis

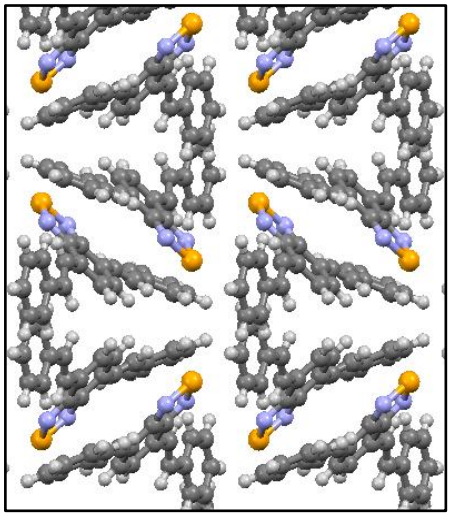

Figure 13: Interlock crystal packing in compound **19** along c-axis

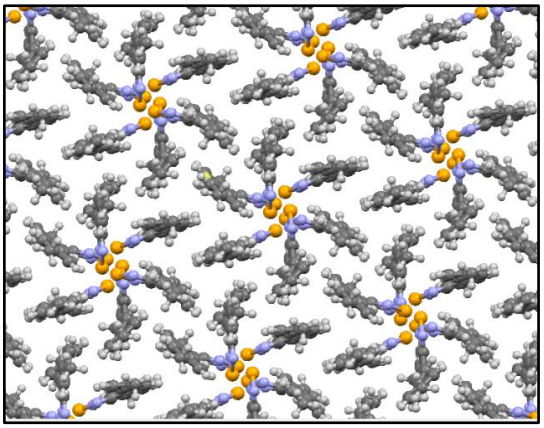

Figure 14: Clockwise rotating mill liked packing in compound **22** along ac-axis

Apart from this, single crystal X-ray structural characterization of compound **23** was also performed as shown in Figure 15, which confirmed the trans orientation of the vinyl linkage between BTD units and pyridine on both sides. Moreover, it is seen that water molecule is linked between two molecules through vinyl nitrogen. S---N interaction between two molecules have also been observed. Compounds **18, 19** and **22** get arranged *anti* to benzochalcogen ring, whereas compound **23** get packed in *syn* fashioned.

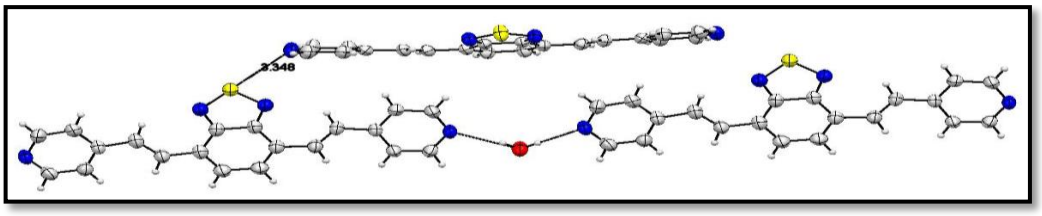

Figure 15: Packing in compound **23**

The inter planer angle for compound **16** was found to be 26.32 as shown in Figure 16.

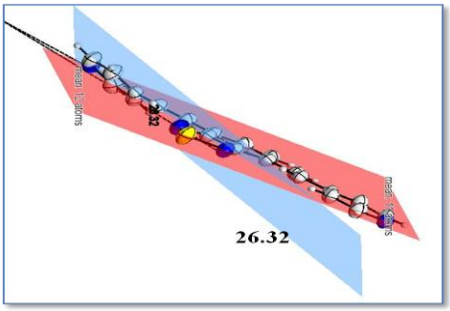

Figure 16

Co-crystals can be defined as multicomponent crystals which are formed by interactions through molecular–recognition-driven assembly processes between different molecular components that exist in single-component crystalline states.[16] Carboxylic acid–

pyridine carboxamide combinations are one of the well-known and well-established co-crystal forming systems.[17] Hydrogen bonding of carboxylic acids with molecules having basic functional groups, such as 4,4'-bipyridine, phenazine, 2-pyridone, and isonicotinamide, results in recognition via acid---pyridine heterosynthon instead of the carboxylic acid dimer.[18] Co-crystal strategies underline the self-assembly of functional compounds which may yield a new generation of multidimensional supramolecular networks due to various intermolecular interactions (hydrogen bonding, π--π stacking interaction, anion--π interaction, and so on)[19]

The preparation of co-crystals **24** were conducted through solution crystallization experiment. It was prepared by mixing the corresponding reactants in 1:2 molar ratio (Compound **23** and terephthalic acid) into a hot methanol solution, and the resulting solution was stirred for approximately half an hour. The product was filtered and recrystallised in dimethyl sulphoxide (DMSO) to get needle like orange crystals of co-crystal **24** as shown in Figure 17. It was observed that after forming co-crystal it becomes almost planer as shown in Figure 18, i.e. interplanar angle was reduced from 26.32 to 1.43. Such type of molecules can become good candidates for application in organic field effect transistors.

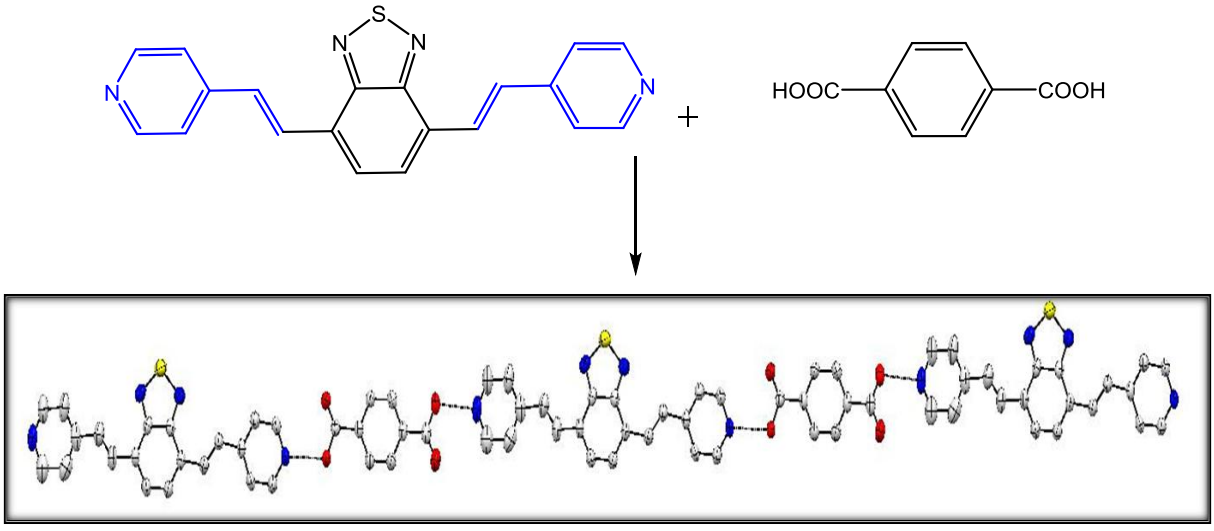

Figure 17: Co-crystal of compound **23** and terephthalic acid

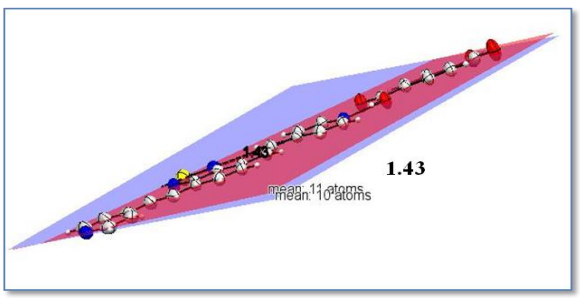

Figure 18

Table 3: Crystallographic data and structures refinement parameters

Identification code	Compound **18**	Compound **19**	Compound **22**	Compound **23**	**(co-crystal)**
Empirical formula	$C_{22}H_{18}N_2S$	$C_{22}H_{16}N_2Se$	$C_{72}H_{60}N_6Se_3$	$C_{40}H_{30}N_8OS_2$	$C_{28}H_{24}N_4O_5S_{0.25}$
Formula weight	342.44	387.33	1246.20	702.87	504.53
Temperature/K	199.94(12)	150.0 (10)	150.00(10)	293(2)	293(2)
Crystal system	monoclinic	monoclinic	triclinic	triclinic	monoclinic
Space group	$P2_1/c$	$P2_1/c$	P-1	P-1	$P2_1/c$
a/Å	9.6081(3)	9.6424(15)	11.8825(6)	9.4466(4)	13.0978(6)
b/Å	15.1360(4)	15.1758(17)	12.7306(5)	9.9176(4)	8.4281(4)
c/Å	11.7745(3)	11.7826(13)	20.6914(8)	19.5777(9)	21.7783(9)
α/°	90.00	90	90.924(3)	79.605(4)	90.00
β/°	101.041(3)	101.61(17)	101.853(4)	86.538(4)	103.164(4)
γ/°	90.00	90	111.378(4)	70.028(4)	90.00
Volume/$Å^3$	1680.64(8)	1688.9(4)	2838.3(2)	1695.58(13)	2340.93(18)
Z	4	4	2	2	4
$\rho_{calc}g/cm^3$	1.353	1.523	1.4581	1.3766	1.432
Crystal size/mm^3	.34× .21 × .15	.35 × .32 × .16	.42 × .23 × .15	.09×.08× .05	.32 × .28 × .25
Radiation	CuKα (λ = 1.54184)	Mo Kα (λ = 0.71073)	Mo Kα (λ = 0.71073)	Cu Kα (λ = 1.54184)	CuKα (λ = 1.54184)
Reflections collected	5794	7713	27620	10879	6730
Independent reflections	3159 [R_{int} = 0.0161, R_{sigma} = 0.0260]	3808 [R_{int} = 0.0628, R_{sigma} = 0.1267]	12985 [R_{int} = 0.0348, R_{sigma} = 0.0624]	6471 [R_{int} = 0.0179, R_{sigma} = 0.0298]	4452 [R_{int} = 0.0197, R_{sigma} = 0.0454]
Data/restraints/parameters	3159/0/226	3808/0/227	12985/0/736	6471/0/468	4452/0/341
Goodness-of-fit on F^2	1.021	1.067	1.021	1.046	1.054
Final R indexes [I>=2σ (I)]	R_1 = 0.0730, wR_2 = 0.1773	R_1 = 0.0961, wR_2 = 0.1747	R_1 = 0.0385, wR_2 = 0.0720	R_1 = 0.0633, wR_2 = 0.1823	R_1 = 0.0749, wR_2 = 0.1957
Final R indexes [all data]	R_1 = 0.0829, wR_2 = 0.1856	R_1 = 0.1731, wR_2 = 0.2183	R_1 = 0.0669, wR_2 = 0.0808	R_1 = 0.0726, wR_2 = 0.1941	R_1 = 0.1047, wR_2 = 0.2210
Largest diff. peak/hole/$eÅ^{-3}$	1.10/-0.86	3.29/-3.24	0.68/-0.78	1.60/-0.55	0.98/-0.30
CCDC Number	1850340	1850346	1850348	1850341	1850342

4.2.2 Application of PANI-Pd in one-pot Wittig-Heck reaction to study effect of R group in dibromobenthiadiazole based molecules

As we have already described in our previous chapter about importance of one-pot multistep synthesis which is found to be a method for the synthesis of wide variety of conjugated molecules. Among various methodologies developed so far, our group has previously reported a variety of olefination reaction involving *in situ* generation of styrene by either one-pot dehydrohalogenation–Heck or one-pot multicomponent Wittig–Heck reaction.[20]

We have used this one-pot Wittig-Heck methodology for the synthesis of stillbene derivatives with dibromobenzthiadiazole; as the drawback for substituted styrenes are difficult to procure or often are unstable at high reaction temperatures or are costly. These type of molecules as seen above, exhibits absorption and fluorescence in the UV-Vis region, which can be widely tuned by chemical functionalization and find wide applications in organic electronics and molecular devices. Here we have taken different substituted aldehydes from electron releasing to withdrawing group and studied its effect by UV-Vis and fluorescence.

4.2.2.1 Synthesis of BDT based conjugated molecules by one-pot Wittig-Heck methodology using PANI-Pd

A series of *p*-substituted benzaldehydes were used which react with methyl triphenyl phosphine iodide to give *in situ* generation of *p*-substituted styrene which will subsequently undergo Mizoroki-Heck reaction with dibromobenzthiadiazole (BDT) in the same pot in presence of PANI-Pd to give final products as shown in scheme 7.

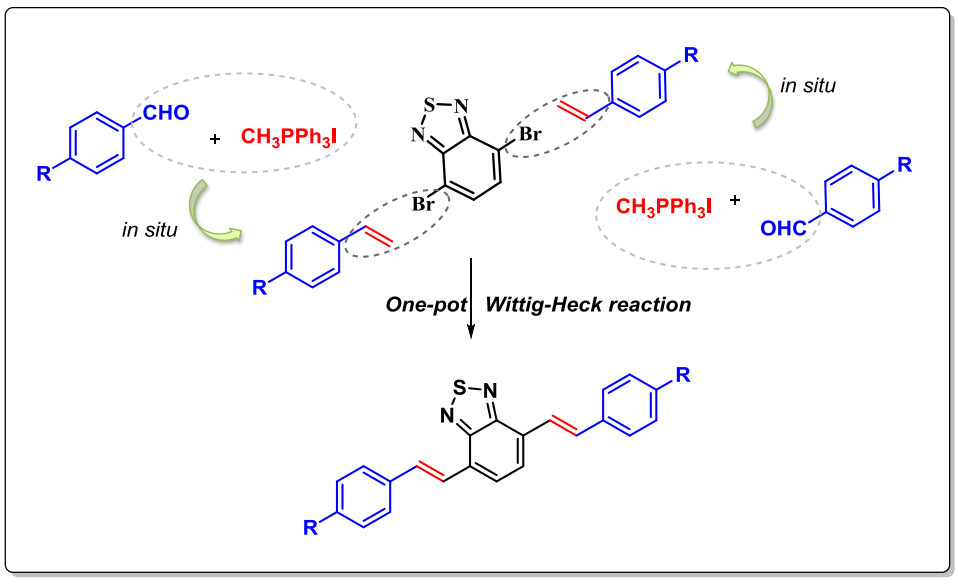

Scheme 7: General scheme for one-pot Wittig-Heck reaction

A series of compounds **25-32** were synthesized and isolated in good yield as shown in Scheme 8. The stereochemistry is determined in the second step, which favors the formation of *E*-isomer.

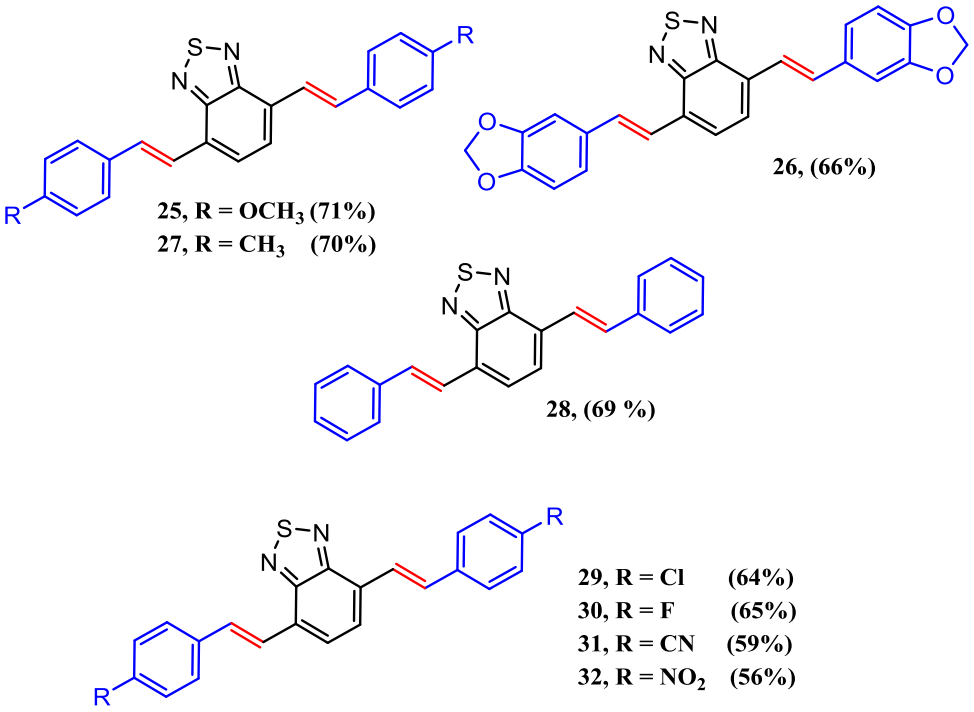

Scheme 8: Molecules prepared by One-pot Wittig-Heck reaction

4.2.2.2 Effect of R group shown by Absorption and Emission spectra of synthesized compounds:

The optical properties of all the synthesized π - conjugated fluorescent molecules were investigated using UV-visible and fluoroscence spectroscopy. The only difference in the terminal functional group shows distinct variation in its optical properties. We have determined that all the compounds in our study are of *E–E* isomers as established by ^{1}H NMR analysis. Figure 19 shows photograph taken under 365 UV lamp in chloroform solution.

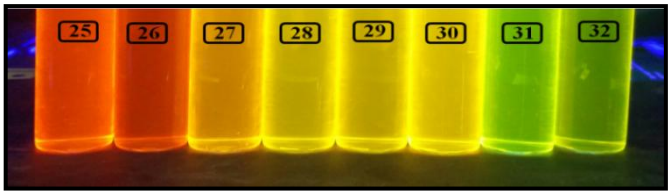

Figure 19: Compounds **25** to **32** as viewed under UV light in solution

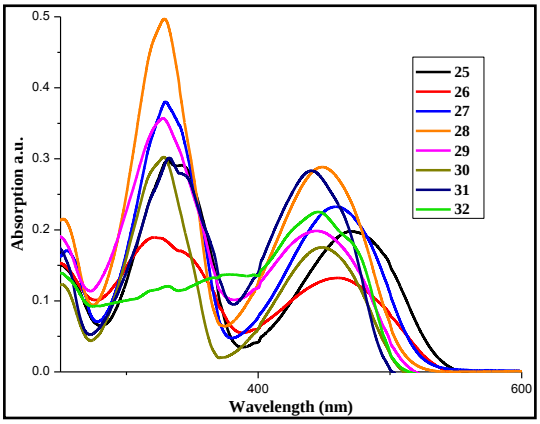

Figure 20: Absorption Spectra of compounds **25-32**

All the absorption and emission spectra were studied in chloroform solution with concentration of 10^{-5} M solution. The absorption near 300 nm does not show much changes which can be assigned to $\pi \rightarrow \pi^*$ electronic transition while the absorption band near 450 nm show changes which can be due to $n \rightarrow \pi^*$ transition as shown in Figure 20. Compound **25** having electron releasing group shows absorption peak at 472 nm whereas that for compound **32** with nitro group shows peak at 446 nm; exhibiting a blue shift of 26 nm as shown in Table 2. Further spectral examination indicates that the λ_{em} for compounds **25-32** varied in the range of 88 nm, that is, from 513 nm for most electron releasing group (R = OCH_3) to 601 nm for most electron withdrawing group (R= NO_2) as shown in Figure 21 and Table 4.

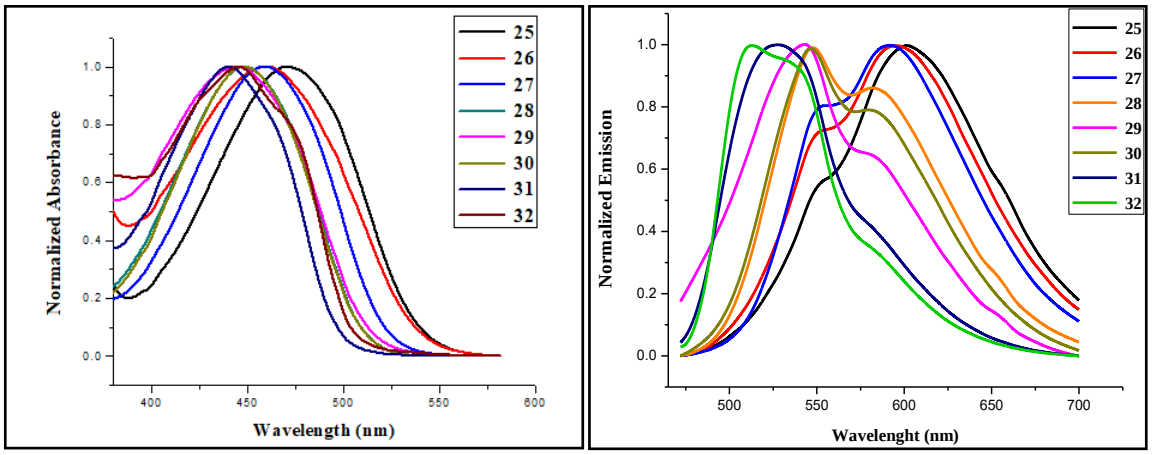

Figure 21: Normalized Absorption and Emission Spectra of compounds **25-32**

Table 4: UV-vis, fluorescence and some electrochemical data for compounds 25-32

Compound	λ_{max} Absorbance nm	λ_{max} Emission nm	λonset	Stoke shift nm	Log ε	E_{gap}^{op} (ev)
25	472	601	555	129	4.30	2.16
26	460	596	568	136	4.12	2.14
27	459	591	536	132	4.37	2.25
28	449	548	520	99	4.46	2.34
29	445	543	527	98	4.30	2.31
30	448	546	523	98	4.24	2.32
31	440	528	503	88	4.45	2.48
32	446	513	516	67	4.35	2.39

4.2.2.3 Single crystal X-ray Diffraction (SCXRD) of some of the compounds:

The molecular structures of compounds **26** and **30** are shown in Figure 22. Compound **26** get crystallised into triclinic crystal system with P-1 space group while compound **30** gets crystallised into monoclinic crystal system with space group Pc (for 1) and P21/c. The molecular packing of compound **30** follows similar crystal packing structure as compound **18** and **19**. Intermolecular supramolecular interactions such as π---π, CH----F, S----F and CH----π favours the interlock type of packing. Due to such stacking, both compounds get arranged anti to each other.

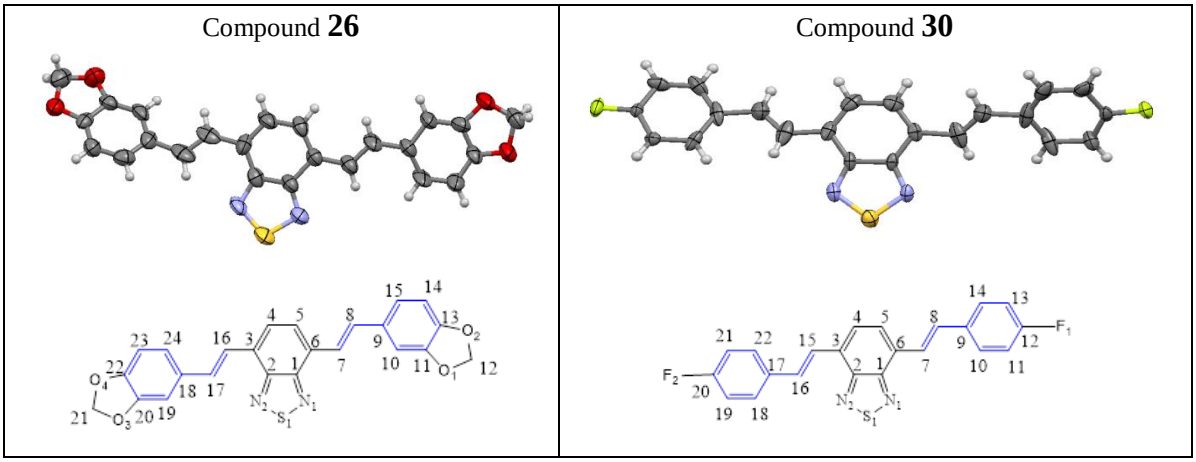

Figure 22: Molecular structures of compounds **26** and **30**

Compounds **26** and **30** are not planar due to substitution on the phenyl ring compared to non substituted ones. Compound **26** forms a rectangular 2D crystal packing due to non-

planarity of phenyl rings as shown in Figure 23. In compound **30**, two fluoro forms a supramolecular interaction with sulphur atom of benzthaidiazole (3.11 and 3.0Å) as well as showing phenyl CH-----F interaction with neighboring molecule forming 1-D ribbon like structure as shown in Figure 24 (along c-axis).

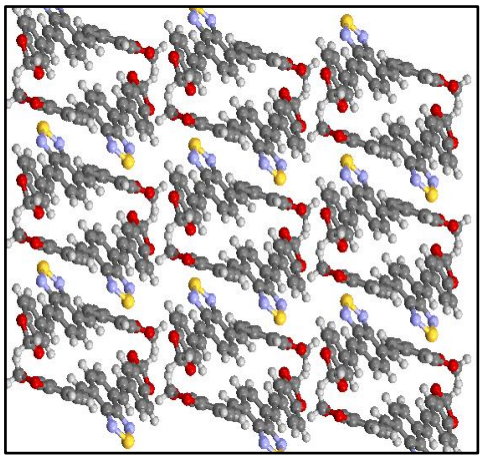

Figure 23: 2-D rectangular crystal packing along c-axis in compound 26

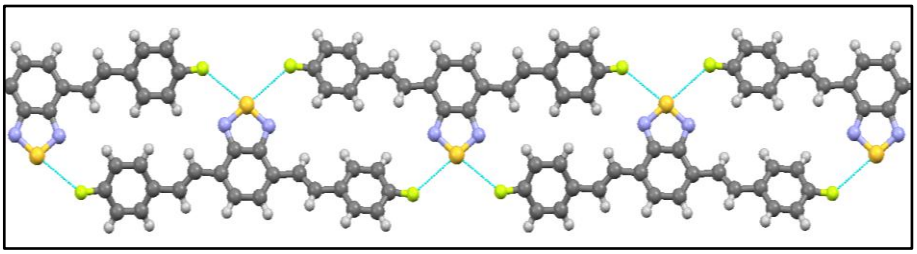

Figure 24: 1-D ribbon like structure of compound **5** along c-axis

Table 5: The selected bond lengths and angles of compound 26 and 30

	Bond Length		*Bond Angles*	
Compound **26**	*N1---S1*	1.641	*N1-S1-N2*	102.28
	N2---S1	1.605	*C6-C7-C8*	124.84
	C7---C8	1.326	*C9-C8-C7*	126.85
	C15---C16	1.280	*C3-C16-C17*	128.93
	O4---C21	1.430	*C18-C17-C16*	122.51
	O3---C21	1.413	*O1-C12-O2*	109.02
	O1---C12	1.439	*O3-C21-O4*	108.32
	O2---C12	1.405		
Compound **30**	*N1---S1*	1.611	*N1-S1-N2*	101.13
	N2---S1	1.610	*C6-C7-C8*	128.06
	C7---C8	1.259	*C9-C8-C7*	123.08
	C15---C16	1.261	*C3-C15-C16*	126.99
	F1---C12	1.345	*C17-C16-C15*	126.46

Table 6: Crystallographic data and structures refinement parameters

Identification code	Compound **26**	Compound **30**
Empirical formula	$C_{24}H_{16}N_2O_4S$	$C_{22}H_{14}F_2N_2S$
Formula weight	428.47	376.43
Temperature/K	293(2)	149.98(10)
Crystal system	triclinic	monoclinic
Space group	P-1	$P2_1/c$
a/Å	8.8200(19)	9.5114(10)
b/Å	10.9047(16)	15.6910(17)
c/Å	10.9265(19)	11.5516(11)
α/°	76.670(14)	90
β/°	67.630(18)	98.966(9)
γ/°	89.677(14)	90
Volume/$Å^3$	941.7(3)	1702.9(3)
Z	2	4
$\rho_{calc}g/cm^3$	1.5110	1.4681
Crystal size/mm^3	.42 × .23 × .15	0.42×0.23× 0.15
Radiation	Mo Kα (λ = 0.71073)	Mo Kα (λ = 0.71073)
Reflections collected	20429	7888
Independent reflections	4611 [R_{int} = 0.2856, R_{sigma} = 0.4136]	3893 [R_{int} = 0.0273, R_{sigma} = 0.0414]
Data/restraints/parameters	4611/0/280	3893/0/244
Goodness-of-fit on F^2	0.933	1.066
Final R indexes [I>=2σ (I)]	R_1 = 0.1132, wR_2 = 0.2178	R_1 = 0.1213, wR_2 = 0.3057
Final R indexes [all data]	R_1 = 0.3780, wR_2 = 0.3364	R_1 = 0.1595, wR_2 = 0.3486
Largest diff. peak/hole/$eÅ^{-3}$	1.91/-1.55	0.57/-1.05
CCDC Number	--	1850345

4.3 Conclusion

We have synthesized and characterized various π- conjugated fluoroscent molecules using heterogeneous Pd anchored PANI by Suzuki and Heck reaction. With one-pot Wittig-Heck reaction π- conjugated fluorescent molecules were synthesized and effect of R group on benzthiadiazole ring was investigated using UV-Vis and Fluorescence spectroscopy. It was observed that as we go from electron releasing to electron withdrawing group, it exhibited red to blue shift. Such type of molecules can become good candidates in application as dyes, also the electrical band gap values of all the synthesized compounds are in adequate range (2.14 – 2.48 eV) for testing as OLEDs. Crystal study for few newly synthesized compounds shows interesting interaction and packing patterns.

4.4 Experimental section

Oven-dried glassware were used for all reactions with magnetic stirring. Thin Layer Chromatography was performed on silica gel plates quoted on aluminium sheets. The spots were visualized under UV light or with iodine vapor. All reactions were carried out under an inert atmosphere (nitrogen). All the compounds were purified by column chromatography on silica gel (60-120 mesh). NMR Spectra were recorded on Bruker Avance 400 Spectrometer (400 MHz for ^{1}H-NMR, 100 MHz for ^{13}C-NMR) with $CDCl_3$ as solvent and TMS as internal standard. IR spectra were recorded on a Perkin-Elmer FTIR RXI spectrometer as KBr pallets. UV-Visible absorption of all the compounds was measured in chloroform at room temperature on Perkin-Elmer Lambda 35 spectrometer and fluorescence was measured on Jasco FP-6300 spectro fluorometer. Melting points were recorded in Thiele's tube using paraffin oil and are uncorrected. Solvents and chemicals used were purchased from Spectrochem, Sigma-Aldrich Chemicals Limited and used without further purification.

Synthesis of Benzo 1,2,5 oxadiazole 1-oxide **(2)**

To a cooled solution of *o*-Nitroaniline (10 g, 72 mmol) in alcoholic NaOH at 0°C, solution of sodium hypochlorite NaOCl (100 ml) was added dropwise and stirred for 20 min. After that mixture was filtered and washed with water to yield bright yellow solid. The product is directly subjected for next step without purification and drying.

Synthesis of 1,2,5-Benzooxadiazole **(3)**

In a clean dry flask compound **2** (8.8g, 64.7 mmol) in THF was degassed by bubbling nitrogen for 15 mins. To that triethyl phosphite $P(OEt)_3$ (22 mL) was added and stirred at 60°C overnight until the starting material is consumed on TLC. Reaction mixture was quenched extracted in ethylacetate and purified by column chromatography on silica gel to yield pale yellow solid. The combined yield for both steps is 20 %.
M.p.: 50-51^{o}C [Lit[10] 52-53 ^{o}C].

Synthesis of 4, 5, 6, 7-Tetrabromo-4,5,6,7-tetrahydrobenzo 2,1,3-oxadiazole **(4)**

Compound **3** (1 g, 8.33 mmol) was stirred at room temperature with HBr (47%, 8.4 mL) and molecular bromine (2.26 mL) for 32 h. Mixture was then poured to sodium sulfite

solution with stirring until molecular bromine is consumed. Filter and wash the precipitate with water, crude product was purified by recrystallization from ethanol twice or thrice.
M.p.: 141-143 ^{o}C [Lit[10] 143-145 ^{o}C]

Synthesis of 4,7-Dibromo-2,1,3-benzooxadiazole **(5)**

To a stirred solution compound **4** (0.9 g, 2.05 mmol) in THF, 1,8-diazabicyclo[5.4.0]undec-7-ene (DBU) (0.78 mL, 5.13 mmol) was drop-wise added at room temperature. The solution was stirred for 30 mins and poured into HCl (aq. 2N, 20 mL). The solution was extracted with ethylacetate and purified by column chromatography on silica gel to yield product in 70 %, recrystallized was done in methanol if required.
M.P.: 111-113 ^{o}C [Lit[10] 112-112.5 ^{o}C]
^{1}H NMR (400 MHz, $CDCl_3$): δ 7.5 (s, 2H)

Synthesis of 2,1,3-Benzothiadizole **(7)**
Clean dry flask was charged with *ortho* phenylene diamine (5 g, 46.3 mmol) in dichloro ethane (50 mL) and triethyl amine (19.27 mL, 138.9 mmol). To this mixture $SOCl_2$ (8.61 mL, 115.8 mmol) was added dropwise as temperature rises due to exothermicity of the reaction. After complete addition, reaction mixture is refluxed for 8-12 hrs. The cooled reaction mixture is then filtered and the precipitates are washed twice and thrice with DCE and discard them. The combined filterate was reduced under pressure to remove excess of solvent, crude mass is subjected to steam distillation for further purification to give product in 36 % yield.
M.P.: 45 ^{o}C [Lit[11] 45-46 ^{o}C]
^{1}H NMR (400 MHz, $CDCl_3$): δ 7.61-7.63 (dd, J = 6.8, 3.2 Hz, 1H), 8.02-8.05 (dd, J = 7.2, 3.6 Hz, 1H).

Synthesis of 4,7-Dibromo 2,1,3-benzothiadizole **(8)**
Benzthiadizole (5 g, 37 mmol) was stirred with HBr (47 %, 180 mL) as the solvent. To this solution molecular bromine (5.7 mL, 110.3 mmol) and HBr (47%, 51 mL) was added drop-wise using dropping funnel and reflux for 8-10 hrs. Precipitate were filtered and washed with saturated solution of sodium thiosulfate to remove excess of bromine and purify the sample by column chromatography on silica gel to afford product in 89 % yield.
M.P.: 191-194 ^{o}C [Lit[11] 193-194 ^{o}C]
^{1}H NMR(400 MHz, $CDCl_3$): δ 7.73 (s, 1H).

3,6-dibromobenzene-1,2-diamine **(9)**

In a dry round bottom flask 4,7-Dibromo 2,1,3-benzothiadizole (0.7 g, 2.38 mmol), was dissolved in dry THF under nitrogen atmosphere. $LiAlH_4$ (0.45 g, 11.9 mmol) was added in portions at 0^oC and was stirred for 5 h at room temperature. Reaction was quenched with saturated ammonium chloride solution, extractrd in ethyl acetate and purified by column chromatography to afford product in 85 % yield.

M.P.: 101 ^oC [Lit[11] 100-101 ^oC]

^1H NMR (400 MHz,$CDCl_3$): δ 3.92 (br s, 2H), 6.87 (s, 1H)

4,7-dibromobenzo 2,1,3 selenadiazole **(10)**

To a solution of Compound **9** (0.5 g, 1.62 mmol) in 10 ml ethanol solution of SeO_2 in water was added slowly and refluxed for 3 h. The solution was cooled and precipitates were filtered and purified by crystalliton to afford product in 65 % yield.

M.P.: 285-286 ^oC [Lit[11] 285-287 ^oC]

^1H NMR (400 MHz,$CDCl_3$): δ 7.67 (s, 1H)

General procedure for the Suzuki-Miyaura reaction (Scheme 3):

To an oven-dried two necked round bottom flask equipped with a stirrer bar was charged dibromobenzochalcogendiazole (0.2 g, 1 eq.), potassium carbonate (4 eq.), PANI-Pd catalyst (0.12 g, 0.044 mmol of Pd) in dioxane. To the reaction mixture phenyl/thiophene boronic acid (2.5 eq.) was added and was heated at 90-95 ^oC for 20 h. The reaction mixture was quenched with water and extracted with ethyl acetate (3x25 mL). The combined organic phase was washed with water and dried over anhydrous sodium sulfate. Solvent was removed in vacuum and crude product was purified by column chromatography on silica gel to afford biphenyl.

4,7-diphenylbenzo[c][2,1,3]oxadiazole **(11)**

Yield: 87 %

M.p. 188 ^oC [Lit.[21] 190-191 ^oC]

^1H-NMR ($CDCl_3$, 400 MHz): δ 7.49-7.52 (m, 1H), 7.54-7.59 (m, 2H), 7.70 (s, 1H), 8.05-8.07 (m, 2H).

Mass (EI) m/z: 272 (M^+, 100), 239 (47) $cm.^{-1}$

4,7-diphenylbenzo[c][2,1,3]thiadiazole **(12)**

Yield: 83 %

M.p. 125 ^{o}C [Lit.[22] 127 ^{o}C]

^{1}H-NMR ($CDCl_3$, 400 MHz): δ 7.49-7.51 (m, 1H), 7.56-7.60 (m, 2H), 7.82 (s, 1H), 7.94-8.00 (m, 2H).

Mass (EI) m/z: 289 (M+1, 100) cm.$^{-1}$

4,7-diphenylbenzo[c][2,1,3]selenadiazole **(13)**

Yield: 81 %

M.p. 175-177 ^{o}C [Lit.[2] 177 ^{o}C]

^{1}H-NMR ($CDCl_3$, 400 MHz): δ 7.45-7.549 (m, 1H), 7.54-7.58 (m, 2H), 7.65 (s, 1H), 7.89-87.91 (m, 2H).

Mass (EI) m/z: 355 (M^{+}, 37), 255 (100), 227 (28)

4,7-di(thiophen-2-yl)benzo[c][2,1,3]oxadiazole **(14)**

Yield: 78 %

M.p. 121-123^{o}C [Lit.[23] 123-125^{o}C]

^{1}H NMR (400 MHz, $CDCl_3$): δ 7.22-7.24 (m, 2H), 7.46-7.48 (m, 2H), 7.63 (s, 2H), 8.13-8.14 (m, 2H)

^{13}C NMR (100 MHz, $CDCl_3$): δ 122.1, 126.3, 126.9, 128.6, 128.7, 137.9, 147.8

Mass (EI) m/z: 284 (M^{+}, 100), 283 (64), 254 (35).

4,7-di(thiophen-2-yl)benzo[c][2,1,3]thiadiazole **(15)**

Yield: 80 %

M.p. 123-124^{o}C [Lit.[24] 123-125^{o}C]

^{1}H NMR (400 MHz, $CDCl_3$): δ 7.22-7.24 (m, 2H), 7.47-7.48 (m, 2H), 7.88 (s, 2H), 8.13-8.14 (m, 2H).

^{13}C NMR (100 MHz, $CDCl_3$): δ 125.8, 126.0, 126.8, 127.5, 128.0, 139.3, 152.6.

Mass (EI) m/z: 300 (M^{+}, 100), 299 (90).

4,7-di(thiophen-2-yl)benzo[c][2,1,3]selenadiazole (**16**)

Yield: 70 %

M.p. 126^{o}C [Lit.[2] 127 ^{o}C]

^{1}H NMR (400 MHz, $CDCl_3$): δ 7.21-7.23 (m, 2H), 7.48-7.49 (m, 2H), 7.82 (s, 2H), 8.03-8.04 (m, 2H).

^{13}C NMR (100 MHz, $CDCl_3$): δ 126.1, 127.1, 127.4, 127.5, 127.7, 139.6, 158.2.

Mass (EI) m/z: 300 (M^+,100), 299 (90).

General procedure for the Mizoroki-Heck reaction (Scheme 5):

To a dried two neck round bottom flask dibromobenzochalcogendiazole (0.2 g, 1 eq.), PANI-Pd (0.15 g, 0.055 mmol of Pd), dry potassium carbonate (4 eq.) were added. Dry DMA (10 mL) was used as solvent and then solution of styrene (2.5 eq.) was added under nitrogen atmosphere. The reaction mixture was then heated to 120-140 ^{0}C for 40 h. The reaction mixture was quenched with water and extracted with ethyl acetate and dried over anhydrous sodium sulfate. Solvent was removed in vacuum and crude product was purified by column chromatography on silica gel to afford product.

4,7-di((*E*)-styryl)benzo[c][2,1,3]oxadiazole **(17)**

Yield: 74 %

M.p. 185-186 ^{o}C

^{1}H-NMR (400 MHz, $CDCl_3$): δ 7.29-7.36 (m, 3H), 7.41-7.45 (m, 2H), 7.64-7.66 (m, 2H), 8.06-8.10 (d, *J* = 16 Hz, 1H).

^{13}C NMR (100 MHz, $CDCl_3$): δ 123.7, 126.2, 127.1, 128.6, 128.8, 130.1, 135.8, 137.0, 148.3.

Mass (EI) m/z: 324 (M^+,100), 323(73), 295 (44).

4,7-di((*E*)-styryl)benzo[c][2,1,3]thiadiazole **(18)**

Yield: 71 %;

M.p. 178 $^{\circ}$C.

^{1}H NMR (400 MHz, $CDCl_3$): δ 7.32-7.35 (m, 1H), 7.41-7.45 (m, 2H), 7.66-7.70 (m, 3H), 7.73 (s, 1H), 8.00-8.05 (d, *J* = 16.4 Hz, 1H).

^{13}C NMR (100 MHz, $CDCl_3$): δ 124.5, 127.0 (2C), 128.1, 128.8, 129.3, 133.2, 137.5, 154.0.

Mass (EI) m/z: 341 (M+1, 67), 340 (M^+ ,100).

4,7-di((E)-styryl)benzo[c][2,1,3]selenadiazole **(19)**

Yield: 69 %;

M.p. 180-181°C.

^{1}H NMR (400 MHz, $CDCl_3$): δ 7.31-7.34 (m, 1H), 7.40-7.44 (t, *J* = 8 Hz, 2H), 7.65-7.68 (m, 3H), 7.73-7.77 (d, *J* = 16.4 Hz, 1H), 7.88-7.93 (d, *J* = 16.4 Hz, 1H).

^{13}C NMR (100 MHz, $CDCl_3$): δ 124.7, 126.7, 126.9, 128.1, 128.7, 130.8, 132.9, 137.6, 159.6

Mass (EI) m/z: 387 (M^+ 100), 307 (100).

4,7-bis((*E*)-4-methylstyryl)benzo[c][2,1,3]oxadiazole **(20)**

Yield: 72 %;

M.p. 244 °C.

^{1}H NMR (400 MHz, $CDCl_3$): δ 2.41 (s, 3H), 7.23-7.34 (m, 4H), 7.54-7.56 (d, *J* = 8 Hz, 2H), 8.03-8.07 (d, *J* = 16 Hz, 1H).

^{13}C NMR (100 MHz, $CDCl_3$): δ 21.4, 122.9, 126.1, 127, 129.5, 130.7, 134.3, 135.7, 138.7, 148.4.

4,7-bis((*E*)-4-methylstyryl)benzo[c][2,1,3]thiadiazole **(21)**

Yield: 73 %;

M.p. 202 °C.

^{1}H NMR (400 MHz, $CDCl_3$): δ 2.41 (s, 3H), 7.22-7.23 (d, *J* = 8.4 Hz, 2H), 7.57-7.58 (d, *J1* =8 Hz, 2H), 7.62-7.66 (d, *J* = 16.4 Hz, 1H), 7.71 (s, 1H), 7.96-8.00 (d, *J* = 16.4 Hz, 1H).

^{13}C NMR (100 MHz, $CDCl_3$): δ 21.4, 123.5, 126.7, 126.8, 129.2, 129.5, 133.0, 134.7, 138.1, 154.0.

Mass (EI) m/z: 368(M^+ 100), 367 (80)

4,7-bis((*E*)-4-methylstyryl)benzo[c][2,1,3]selenadiazole **(22)**

Yield: 65 %;

M.p. 192-195 °C.

^{1}H NMR (400 MHz, $CDCl_3$): δ 2.40 (s, 3H), 7.22-7.24 (d, *J* = 8 Hz, 2H), 7.56-7.58 (d, *J* = 8 Hz, 2H), 7.68-7.72 (d, *J* = 16.4 Hz, 1H), 7.84-7.88 (d, *J* = 16.4 Hz, 1H).

^{13}C NMR (100 MHz, $CDCl_3$): δ 21.4, 123.8, 126.5, 126.8, 129.5, 130.7, 132.6, 134.8, 138.1, 159.7.

Mass (APCI) m/z: 417(M+1), 418 (M+2)

4,7-bis((*E*)-2-(pyridin-4-yl)vinyl)benzo[c][2,1,3]thiadiazole **(23)**

Yield: 31 %;

M.p. 225-228 °C. [Lit.[8] 230-232 °C]

^{1}H NMR (400 MHz, $CDCl_3$): δ 7.52-7.54 (dd, *J1* = 4.8 Hz, *J2* = 1.6 Hz, 2H), 7.78 (s, 1H), 7.79-7.83 (d, *J* = 16.4 Hz, 1H), 8.04-8.08 (d, *J* = 16.4 Hz, 1H), 8.65-8.67 (dd, *J1* = 4.8 Hz, *J2* = 1.6 Hz, 2H).

^{13}C NMR (100 MHz, $CDCl_3$): δ 121.1, 128.5, 128.7, 129.3, 131.4, 144.6, 150.3, 153.7.

Mass (APCI) m/z: 343(M+1, 100)

4,7-bis((*E*)-2-(pyridin-4-yl)vinyl)benzo[c][2,1,3]selenadiazole **(24)**

Yield: 26 %;

M.p. Above 230°C.

^{1}H NMR (400 MHz, $CDCl_3$): 7.52-7.54 (dd, *J1* = 4.8 Hz, *J2* = 1.6 Hz, 2H), 7.71 (s, 1H), 7.85-7.89 (d, *J* = 16 Hz, 2H), 7.94-8.00 (d, *J* = 16.4 Hz, 1H), 8.64-8.66 (dd, *J1* = 4.8 Hz, *J2* = 1.6 Hz, 2H).

Mass (APCI) m/z: 389(M^+), 391 (M+2, 100)

General procedure for the one-pot Wittigi-Heck reaction (Scheme 8):

A two neck round bottom flask was charged with dibromobenzothiadiazole (0.2 g, 1 eq.), p-substituted aldehydes (2.2 eq), methyl triphenyl phosphonium iodide (2.4 eq.), potassium bicarbonate (12 eq.), PANI-Pd (0.2 g, 0.073 mmol of Pd) in DMA under nitrogen atmosphere. This mixture was slowly heated to 120 °C and continued for 24 h. The reaction mixture was quenched with water and extracted with ethyl acetate (3 x 25 ml). The combined organic phase was washed with water and dried over anhydrous sodium sulphate. Solvent was removed in *vacuum* and the crude product was purified by column chromatography on silica gel to afford stilbene derivatives.

4,7-bis((*E*)-4-methoxystyryl)benzo[c][2,1,3]thiadiazole **(25)**

Yield: 74 %;

M.p. 198-200°C.

^{1}H NMR (400 MHz, $CDCl_3$): δ 2.41 (s, 3H), 7.23-7.25 (d, *J* = 8.4 Hz, 2H), 7.57-7.59 (d, *J* = 8 Hz, 2H), 7.62-7.66 (d, *J* = 16.4 Hz, 1H), 7.71 (s, 1H), 7.96-8.00 (d, *J* = 16.4 Hz, 1H)

^{13}C NMR (100 MHz, $CDCl_3$): δ 123.5, 126.7, 126.8, 129.3, 129.5, 133.0, 134.7, 138.1, 153.9.

4,7-bis((*E*)-2-(benzo[d][1,3]dioxol-5-yl)vinyl)benzo[c][2,1,3]thiadiazol**e (26)**

Yield: 66 %;

M.p. 190-192 °C.

^{1}H NMR (400 MHz, $CDCl_3$): δ 6.03 (s, 2H), 6.85-6.87 (d, *J* = 7.6 Hz, 2H), 7.10-7.12 (dd, *J1* = 8.4, *J2* = 1.6 Hz, 2H),7.23-7.24 (d, *J* = 1.6 Hz, 1 H) 7.62-7.66 (d, *J* = 16.4 Hz, 1H), 7.71 (s, 1H), 7.96-8.00 (d, *J* = 16.4 Hz, 1H)

^{13}C NMR (100 MHz, $CDCl_3$): δ 101.2. 105.7, 108.5, 122.3, 122.9, 126.7, 129.1, 132.1, 132.7, 147.8, 148.3, 153.9.

Mass (APCI) m/z: 429 (M+1), 430 (M+2).

4,7-bis((*E*)-4-methylstyryl)benzo[c][2,1,3]thiadiazole **(27)**

Yield: 75 %;

M.p. 202 °C.

^{1}H NMR (400 MHz, $CDCl_3$): δ 2.41 (s, 3H), 7.22-7.23 (d, *J* = 8.4 Hz, 2H), 7.57-7.58 (d, *J1* = 8 Hz, 2H), 7.62-7.66 (d, *J* = 16.4 Hz, 1H), 7.71 (s, 1H), 7.96-8.00 (d, *J* = 16.4 Hz, 1H).

^{13}C NMR (100 MHz, $CDCl_3$): δ 21.4, 123.5, 126.7, 126.8, 129.2, 129.5, 133.0, 134.7, 138.1, 154.0.

4,7-di((*E*)-styryl)benzo[c][2,1,3]thiadiazole **(28)**

Yield: 74 %;

M.p. 178 °C.

^{1}H NMR (400 MHz, $CDCl_3$): δ 7.32-7.35 (m, 1H), 7.41-7.45 (m, 2H), 7.66-7.70 (m, 3H), 7.73 (s, 1H), 8.00-8.05 (d, *J* = 16.4 Hz, 1H).

^{13}C NMR (100 MHz, $CDCl_3$): δ 124.5, 127.0, 128.1, 128.8, 129.3, 133.2, 137.5, 154.0.

4,7-bis((*E*)-4-chlorostyryl)benzo[c][2,1,3]thiadiazole **(29)**

Yield: 65 %;

M.p. 256-258 °C.

^{1}H NMR (400 MHz, $CDCl_3$): δ 7.38-7.40 (m, 2H), 7.60-7.64 (m, 4H), 7.70 (s, 1H), 7.99-8.03 (d, *J* = 16.4 Hz, 1H)

^{13}C NMR (100 MHz, $CDCl_3$): δ 125.0, 127.3, 128.1, 129.0, 129.2, 132.1, 133.8, 135.9, 153.7.

4,7-bis((*E*)-4-fluorostyryl)benzo[c][2,1,3]thiadiazole **(30)**

Yield: 66 %;

M.p. 235-237 °C.

^{1}H NMR (400 MHz, $CDCl_3$): δ 7.01-7.14 (t, *J* = 8.8 Hz, 2H), 7.55-7.59 (d, *J* = 16.4 Hz, 1H), 7.63-7.66 (m, 2H), 7.70 (s, 1H), 7.98-8.02 (d, *J* = 16.4 Hz, 1H).

^{13}C NMR (100 MHz, $CDCl_3$): δ 115.7, 115.8, 124.3, 127.0, 128.4, 128.5, 129.2, 132.1, 132.6, 153.9, 161.4, 163.9.

Mass (APCI) m/z: 377(M+1), 378(M+2).

4,4'-((1*E*,1'*E*)-benzo[c][2,1,3]thiadiazole-4,7-diylbis(ethene-2,1-diyl))dibenzonitrile **(31)**

Yield: 64 %;

M.p. 270-272°C.

^{1}H NMR (400 MHz, $CDCl_3$): δ 7.70-7.76 (m, 6H), 8.10-8.15 (d, *J* = 16.4 Hz, 1H)

^{13}C NMR (100 MHz, $CDCl_3$): δ 111.2, 118.9, 127.3, 127.9, 128.2, 129.3, 132.0, 132.6, 141.8, 153.8.

4,7-bis((*E*)-4-nitrostyryl)benzo[c][2,1,3]thiadiazole **(32)**

Yield: 60 %;

M.p. 220-222°C.

^{1}H NMR (400 MHz, $CDCl_3$): δ 7.75-7.79 (d, *J* = 16.4 Hz, 1H), 7.79-7.82 (m, 3H), 8.19-8.23 (d, *J* = 16.4 Hz, 1H), 8.29-8.31 (m, 2H)

^{13}C NMR (100 MHz, $CDCl_3$): δ 124.3, 127.4, 128.6, 129.4, 131.8, 131.9, 143.8, 149.5, 153.7

Spectral data:

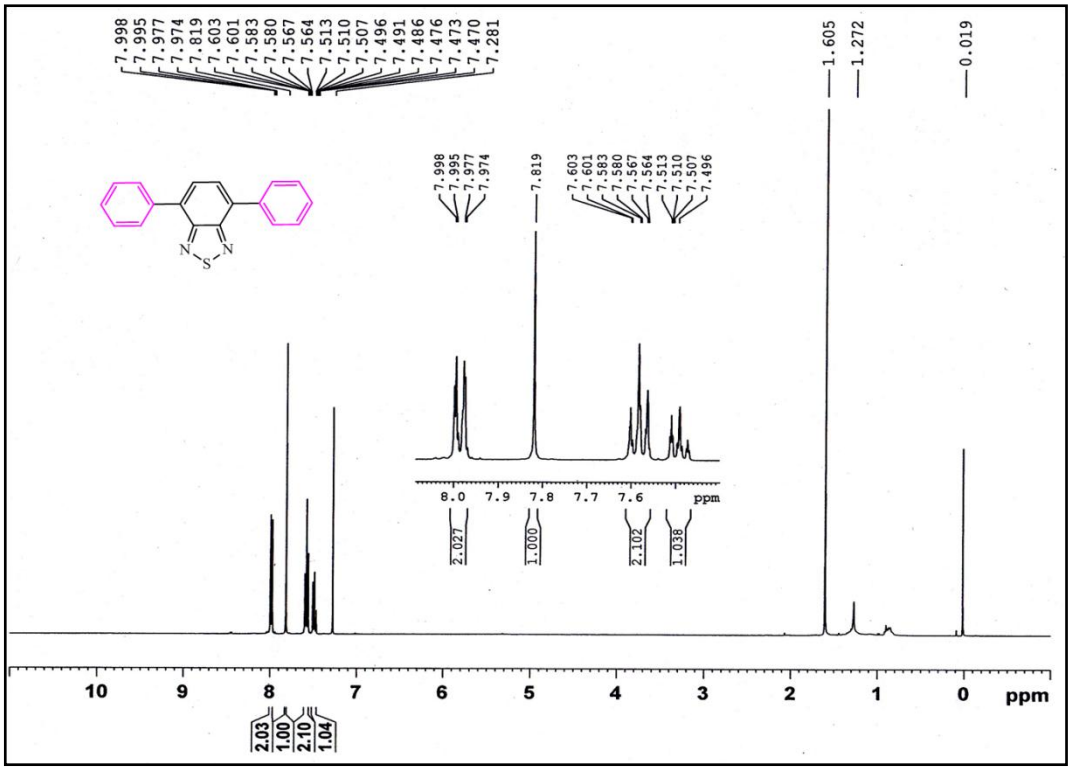

^{1}H-NMR of Compound **12**

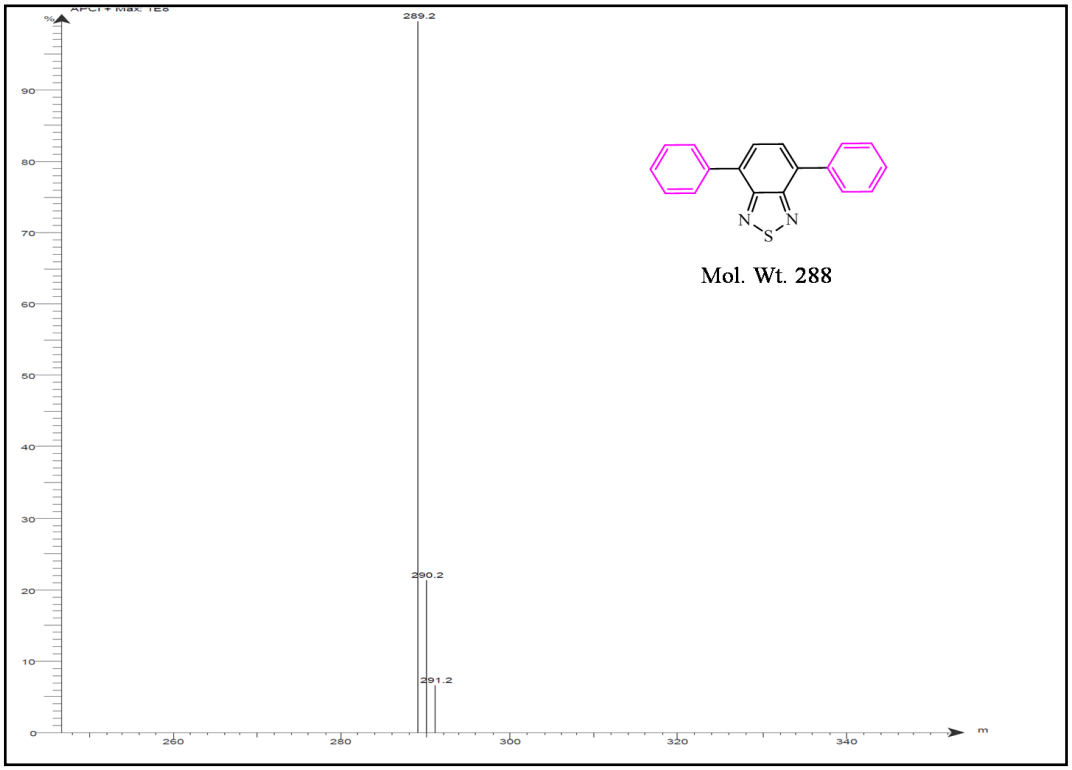

Mass Spectra of Compound **12**

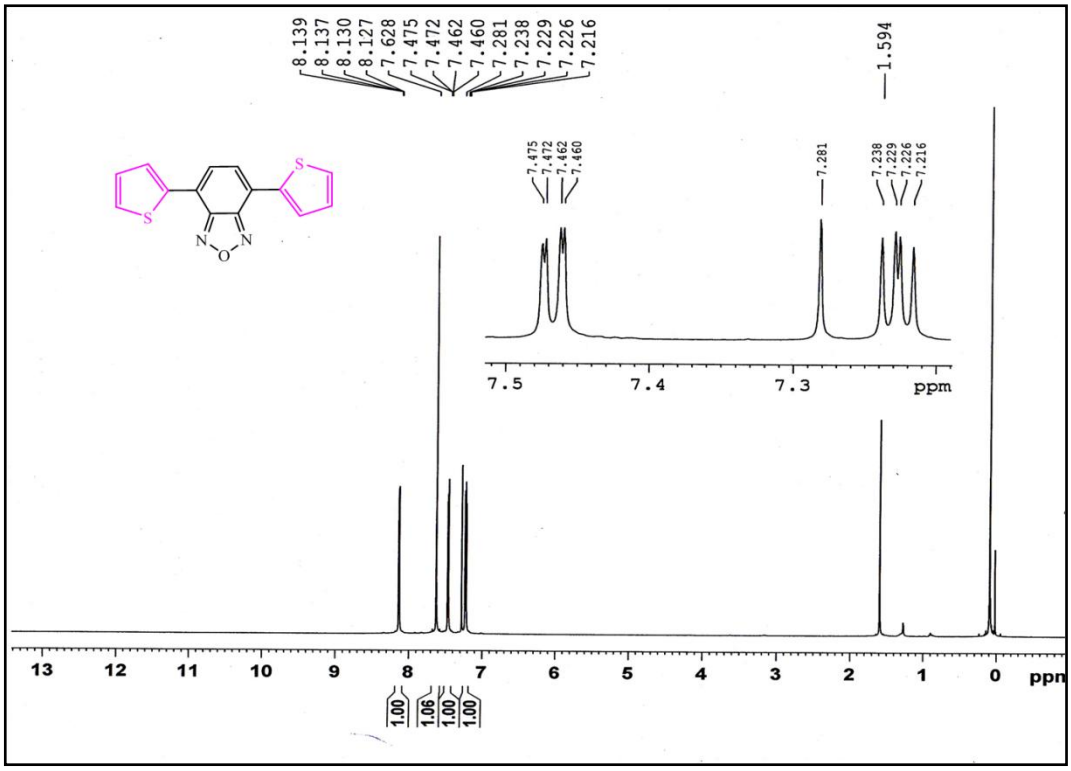

^{1}H-NMR of Compound **14**

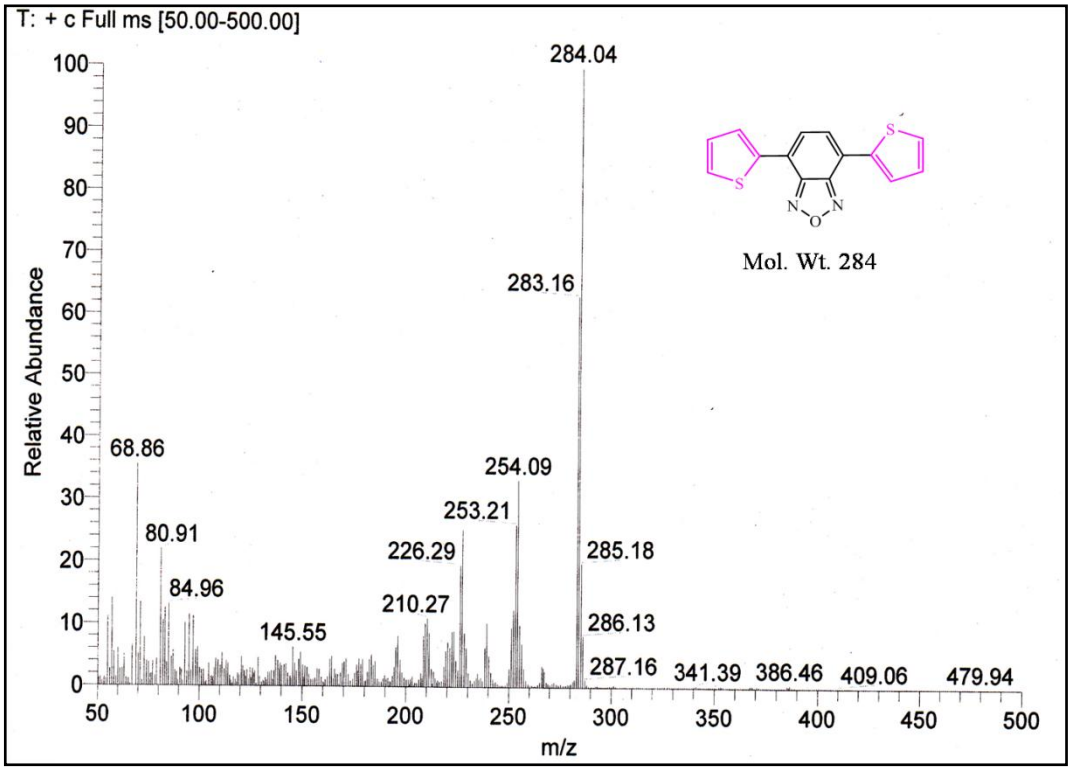

Mass Spectra of Compound **14**

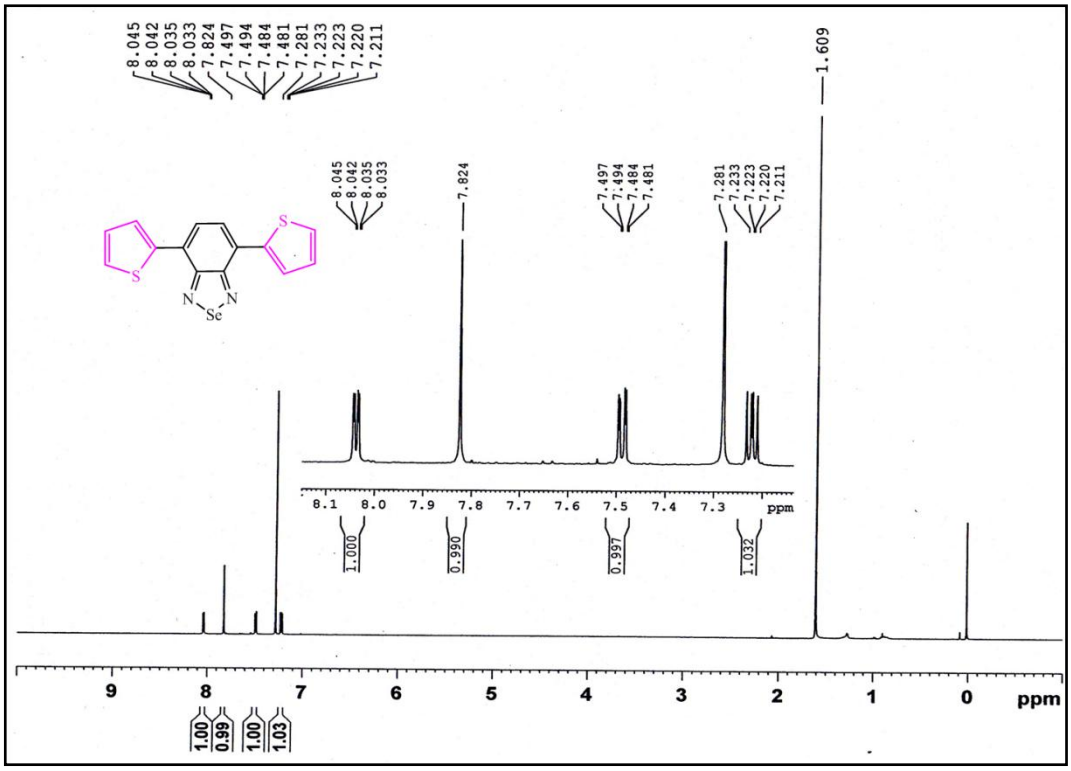

^{1}H-NMR of Compound **15**

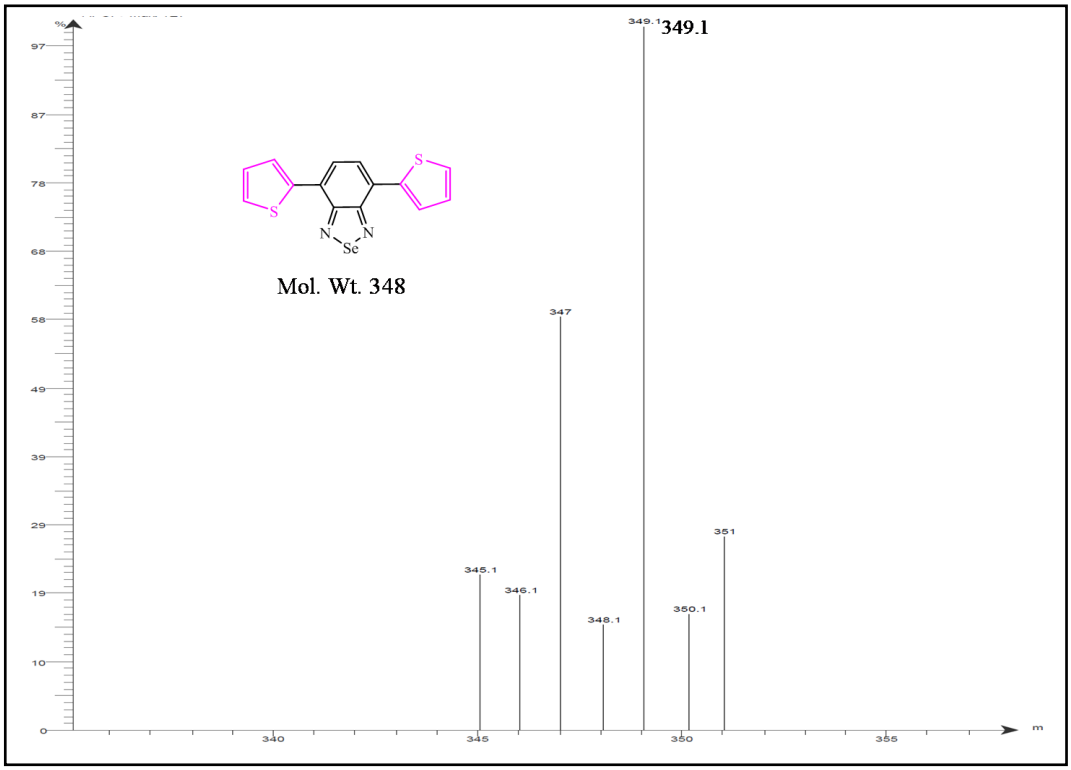

Mass Spectra Of Compound **15**

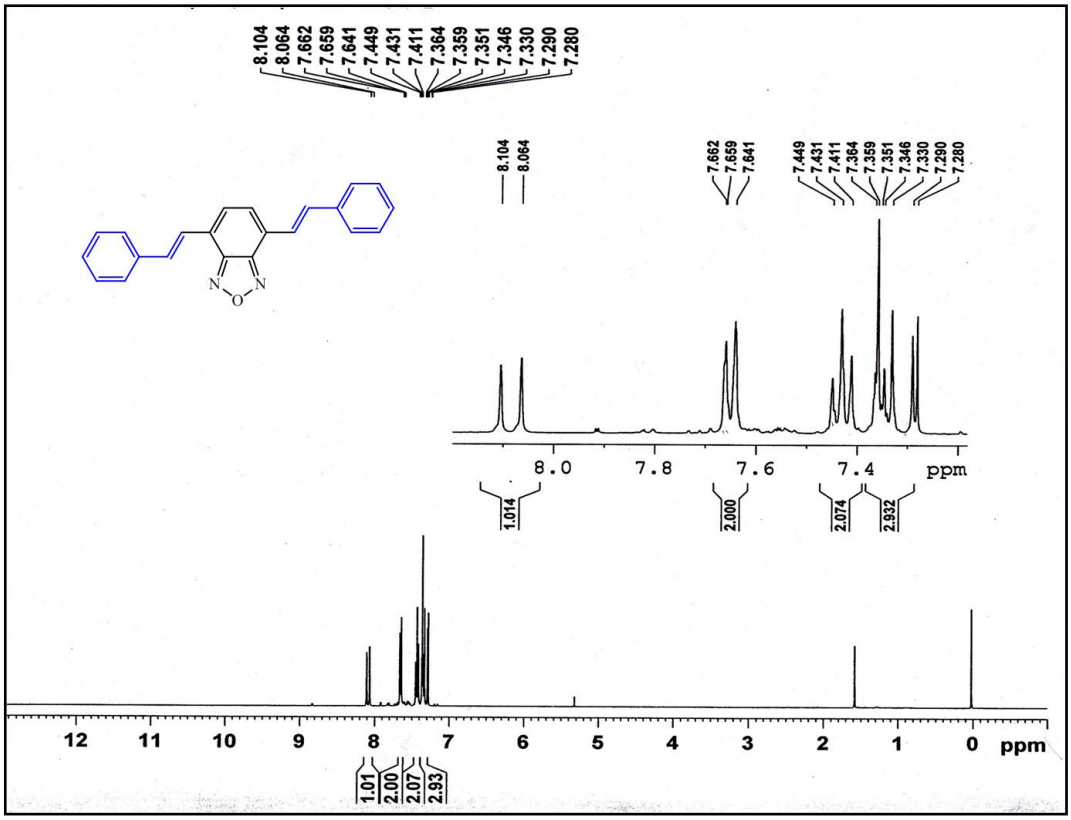

^{1}H-NMR of Compound **17**

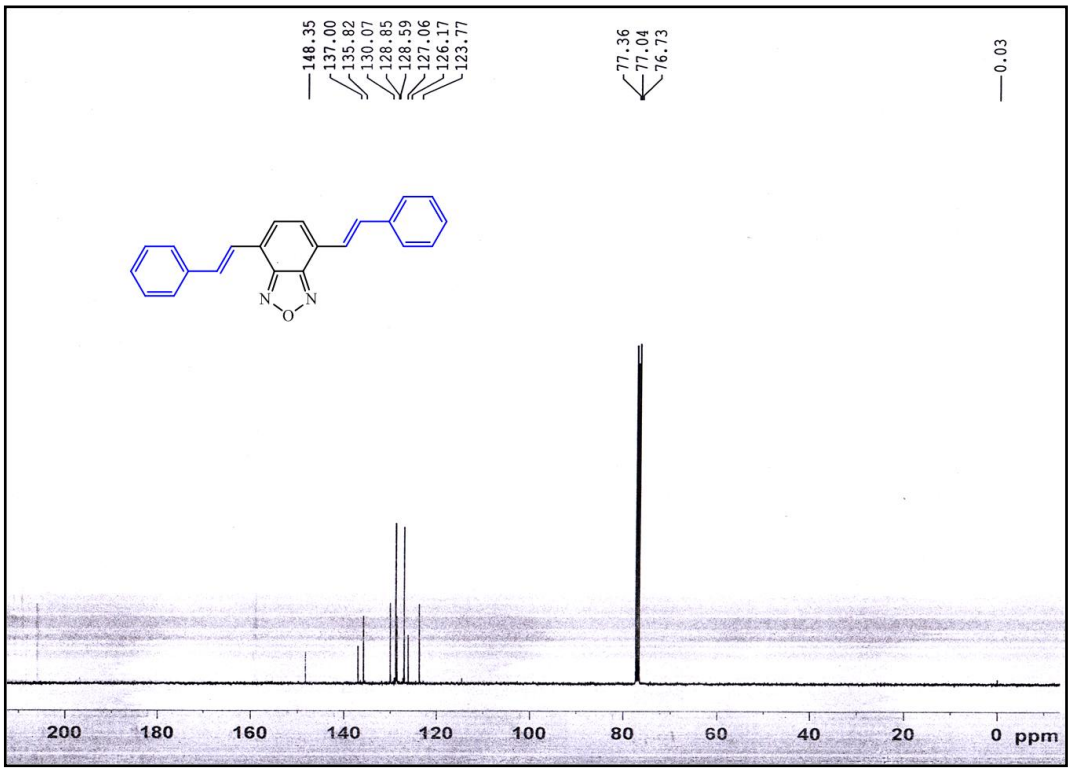

^{13}C-NMR of Compound **17**

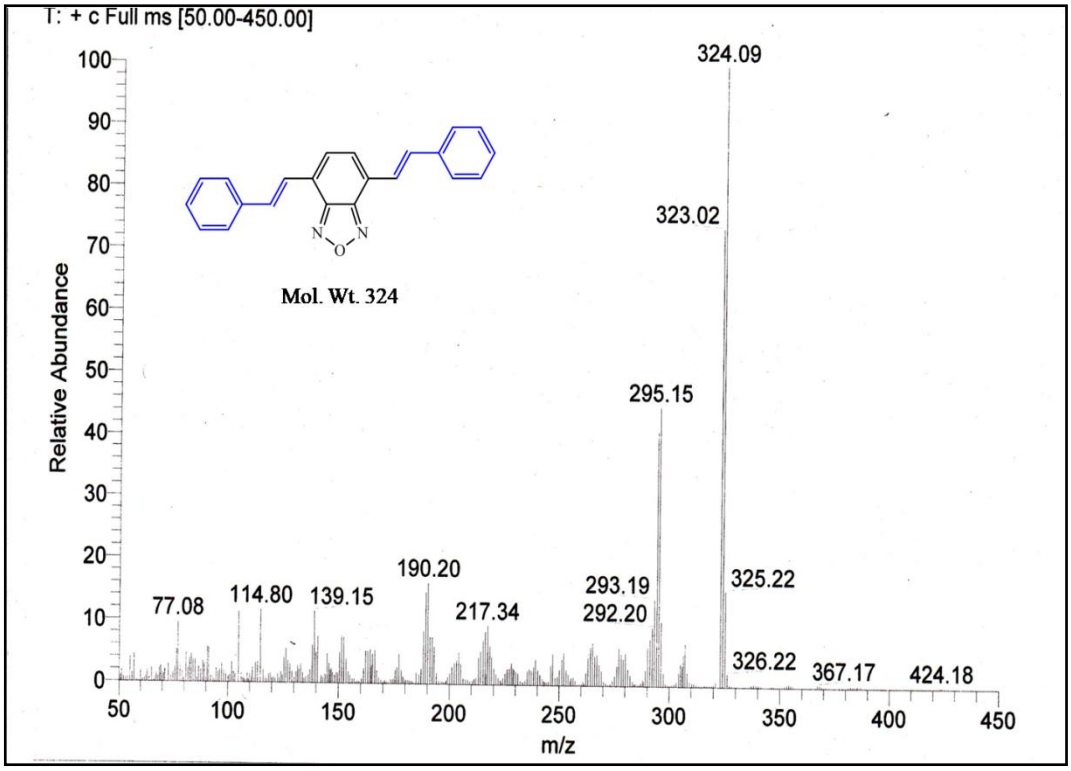

Mass Spectra of Compound **17**

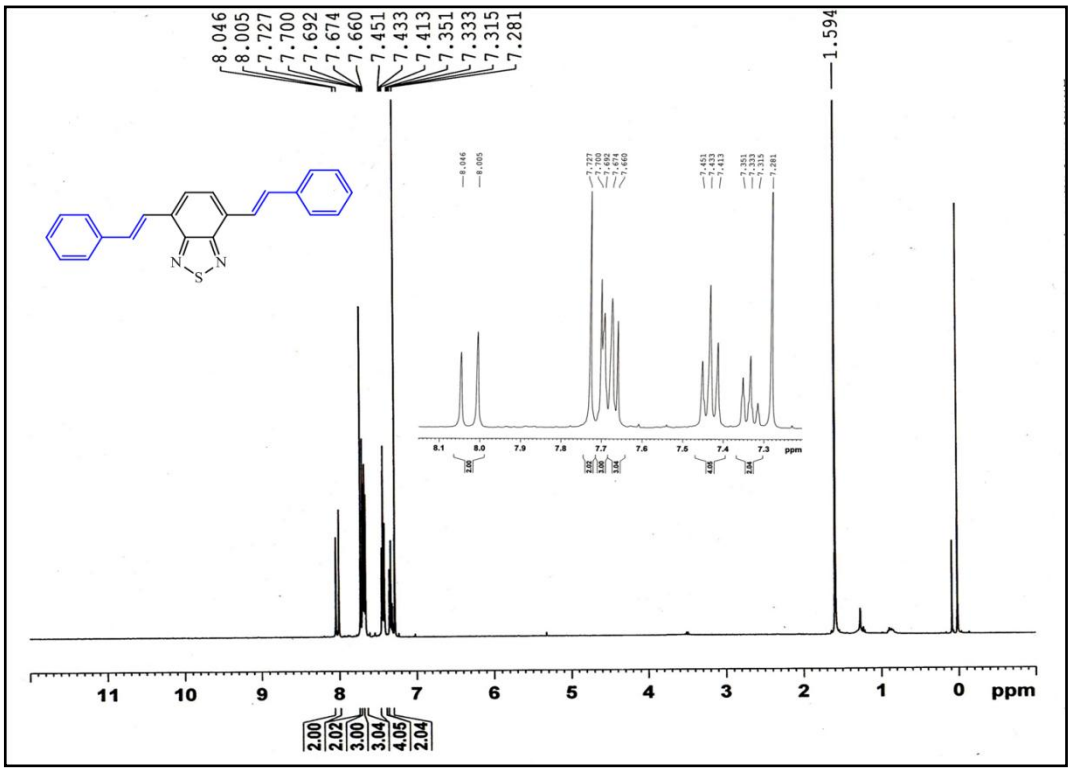

^{1}H-NMR of Compound **18**

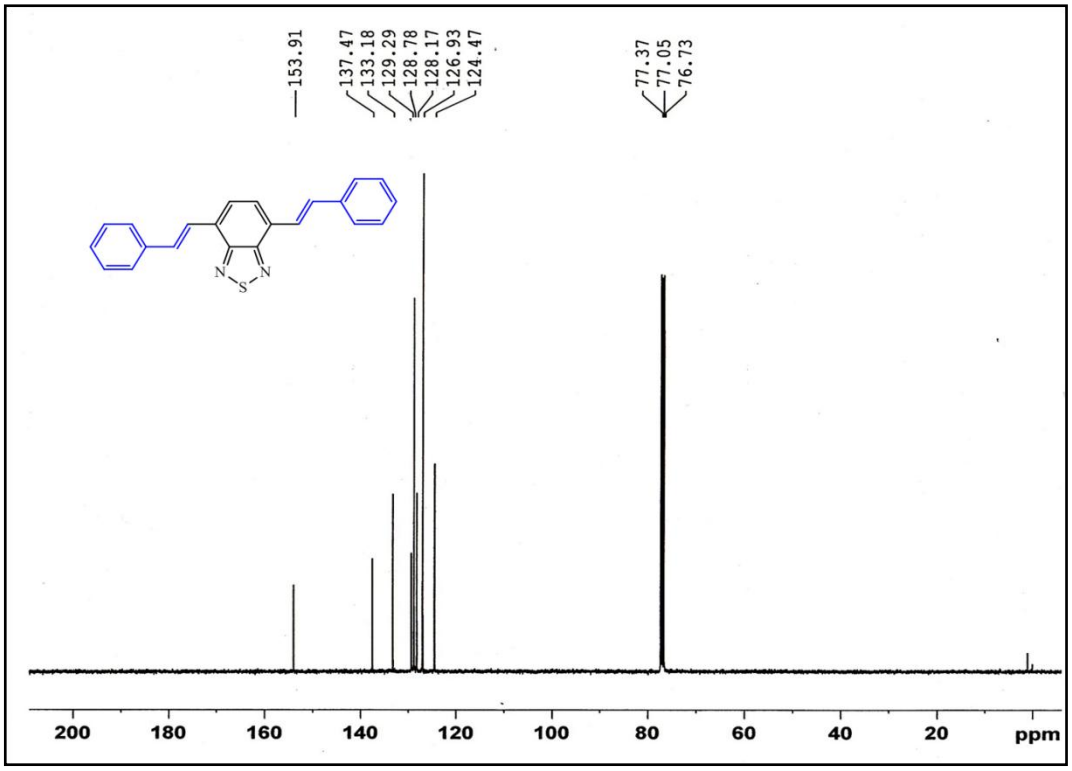

^{13}C-NMR of Compound **18**

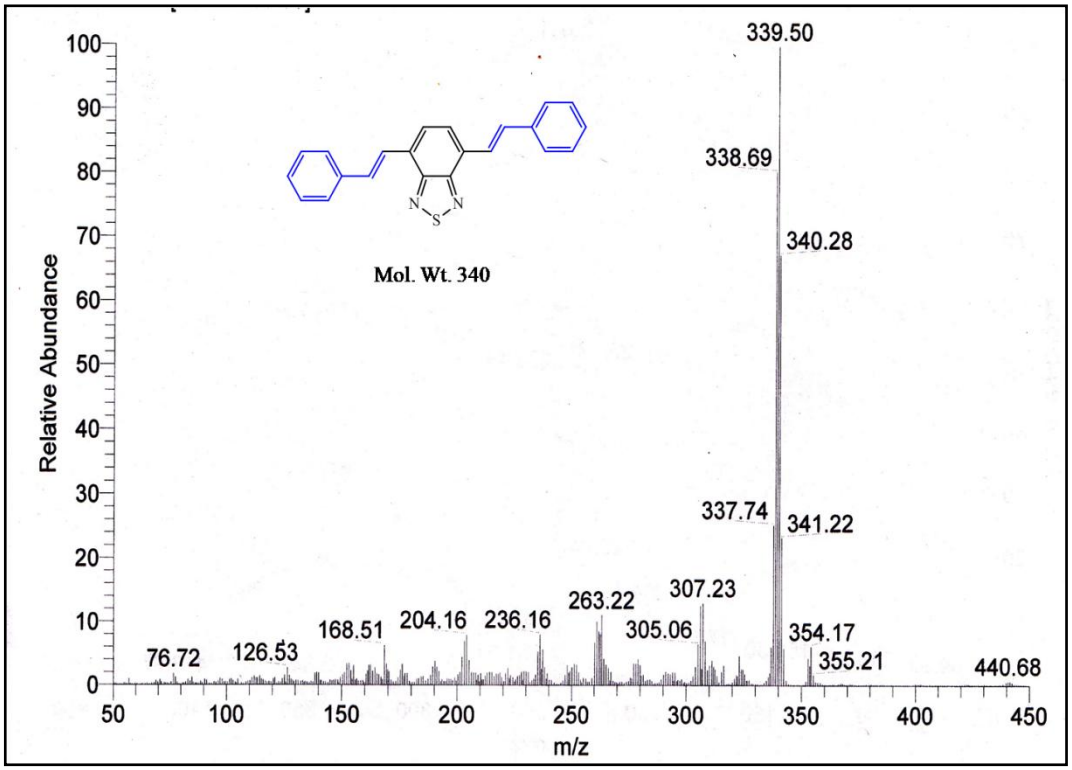

Mass Spectra of Compound **18**

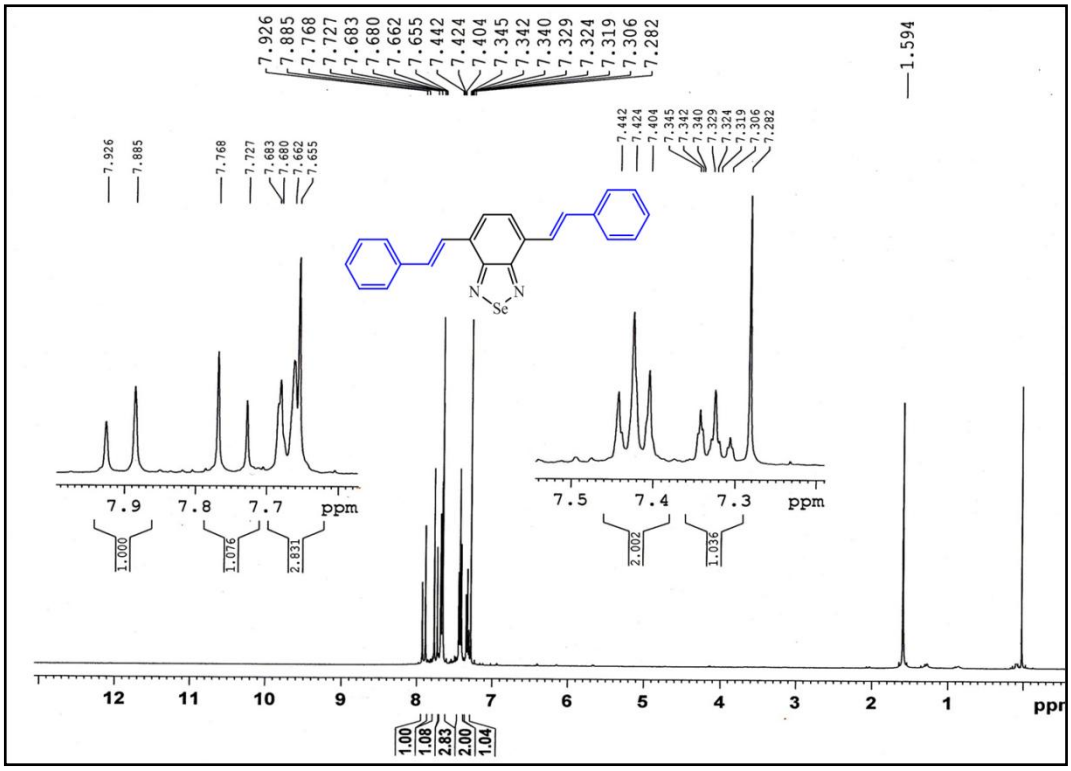

^{1}H-NMR of Compound **19**

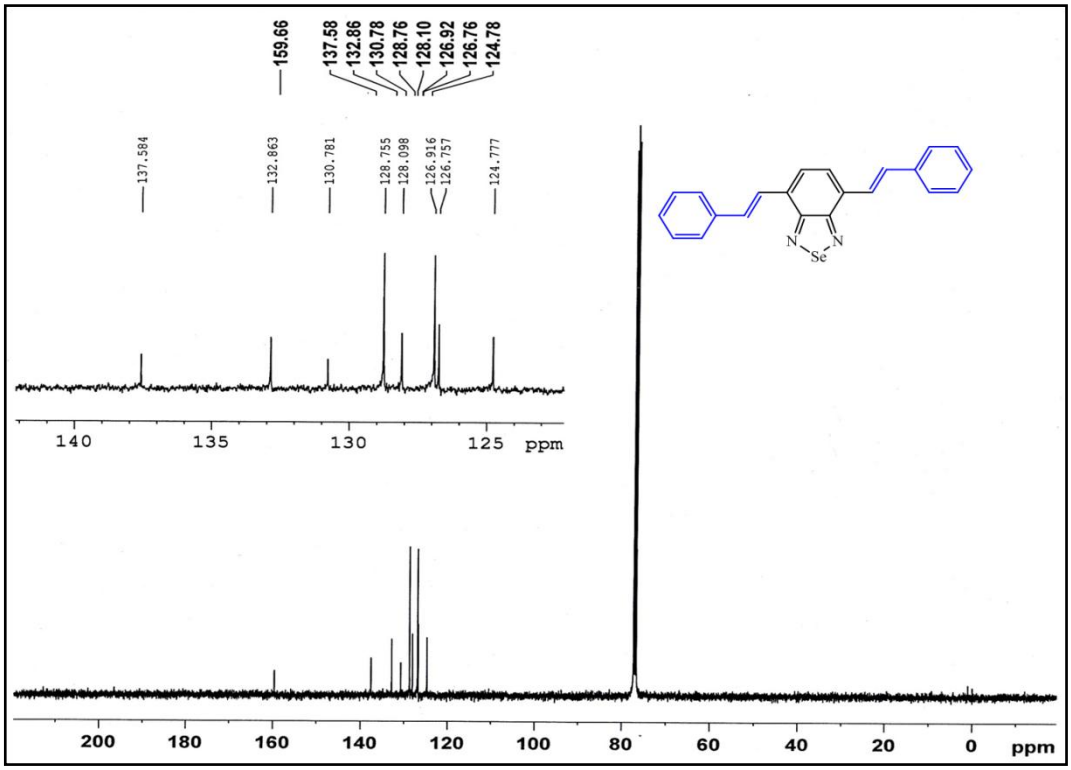

^{13}C-NMR of Compound **19**

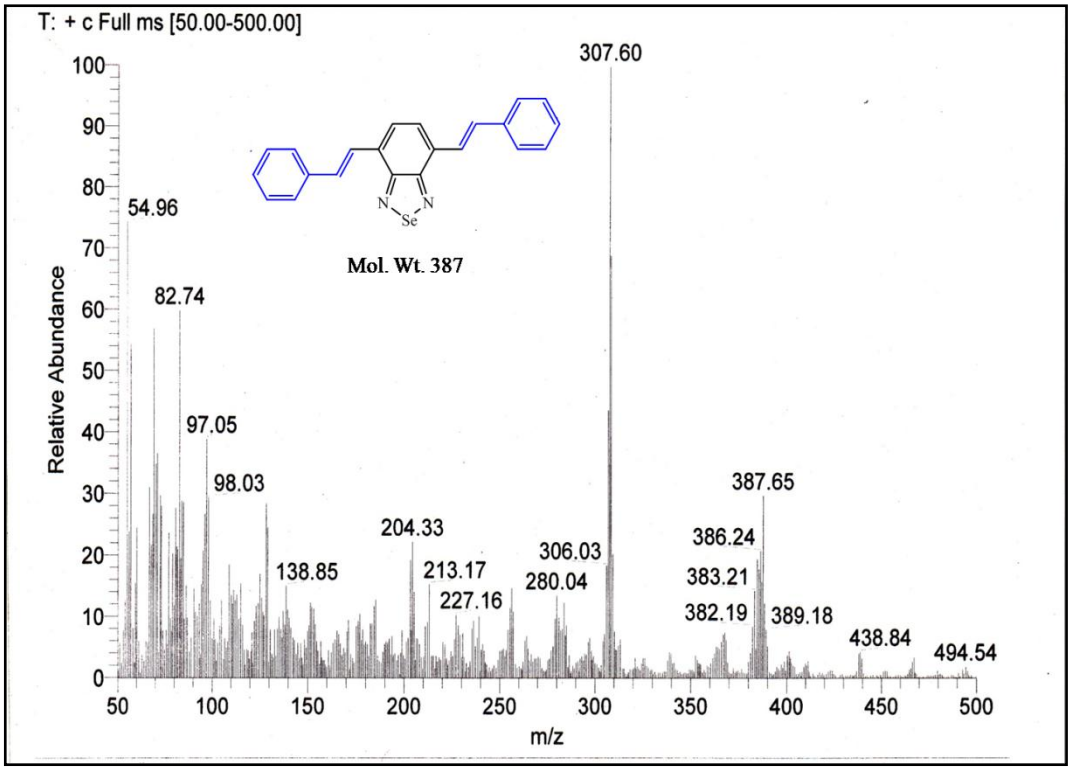

Mass Spectra of Compound **19**

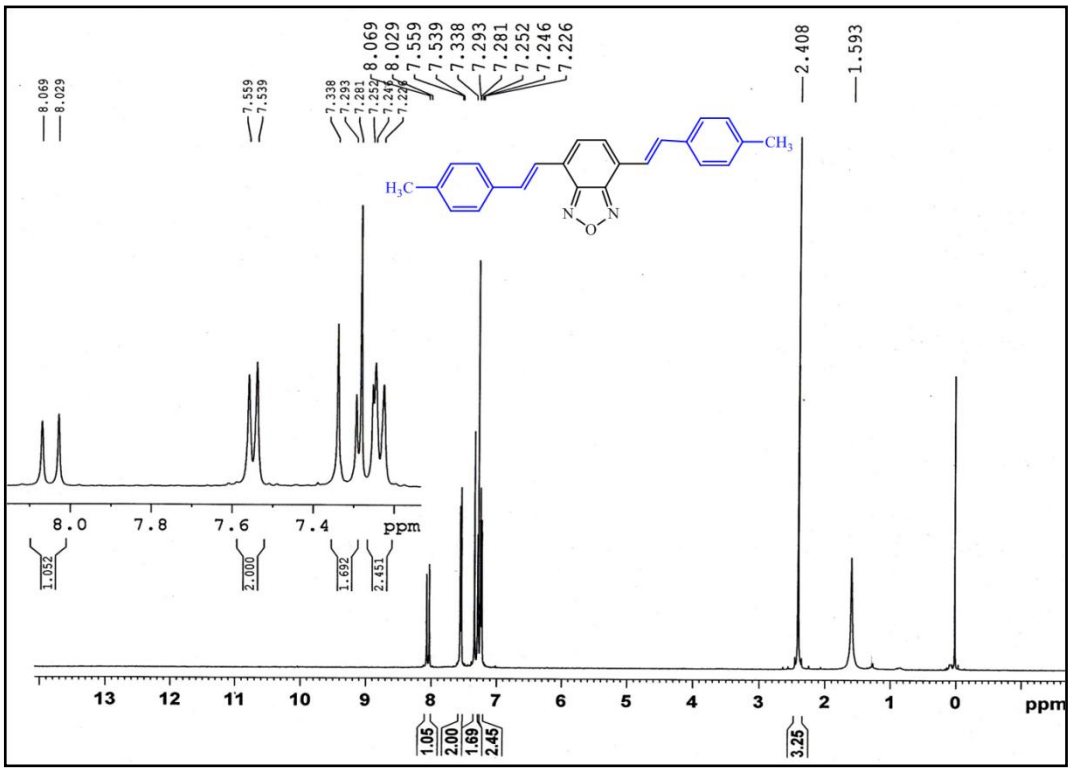

^{1}H-NMR of Compound **20**

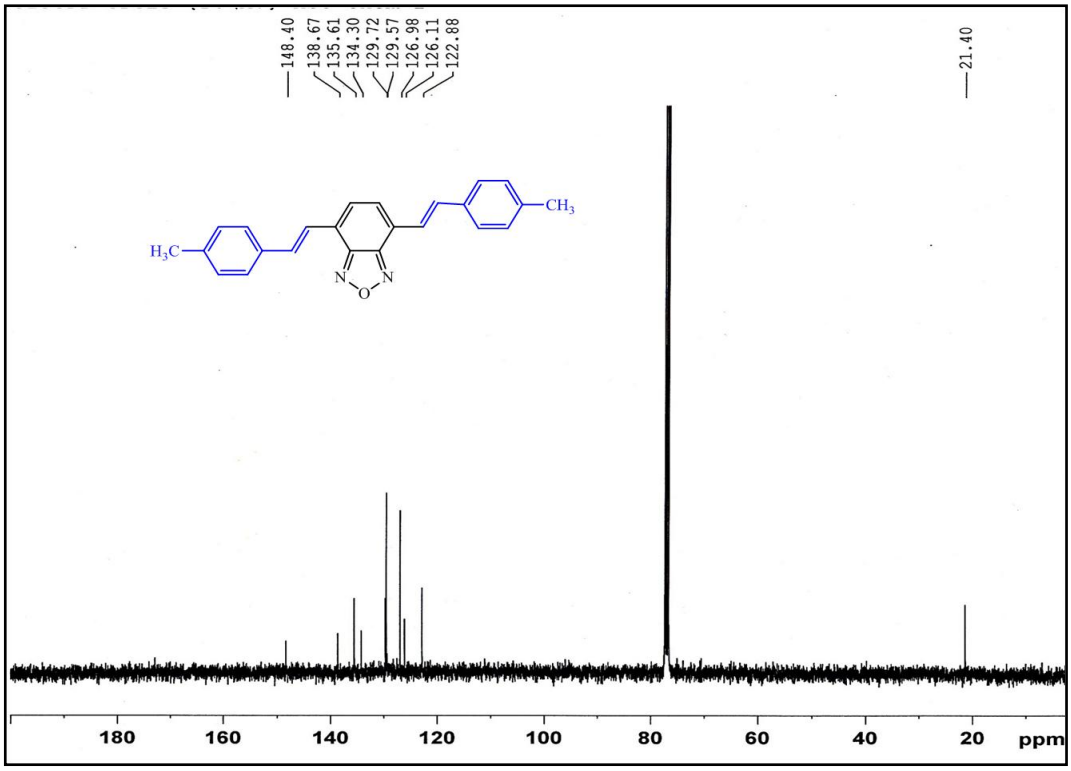

^{13}C-NMR of Compound **20**

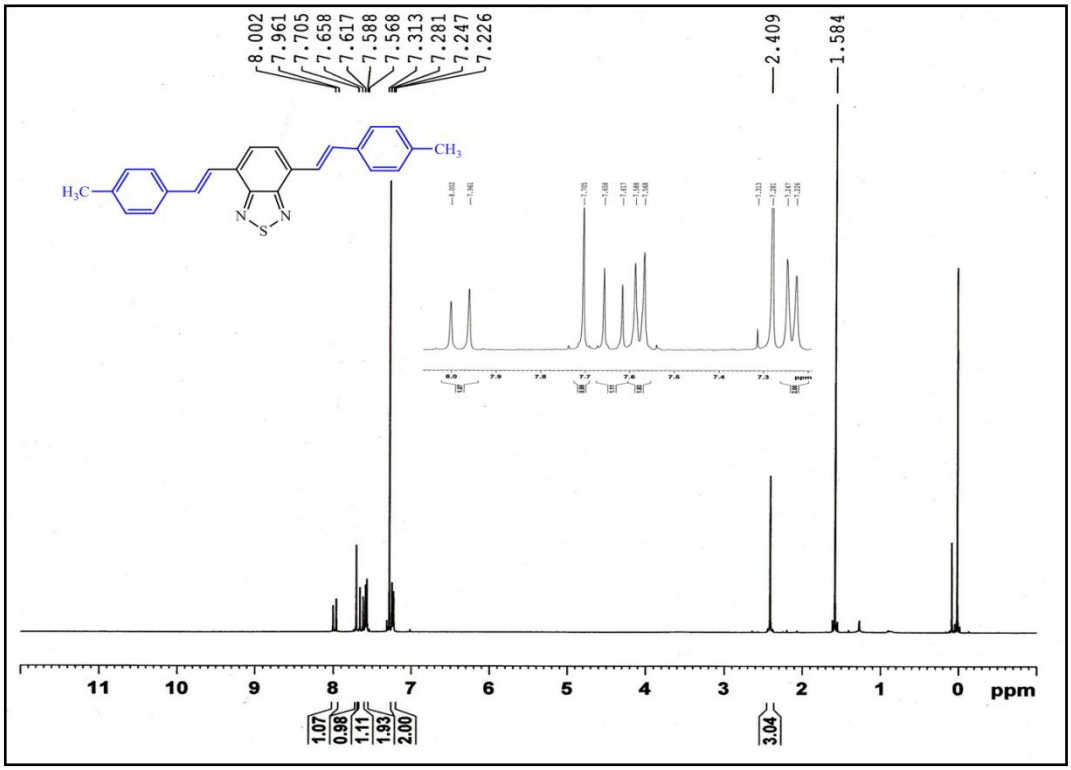

^{1}H-NMR of Compound **21**

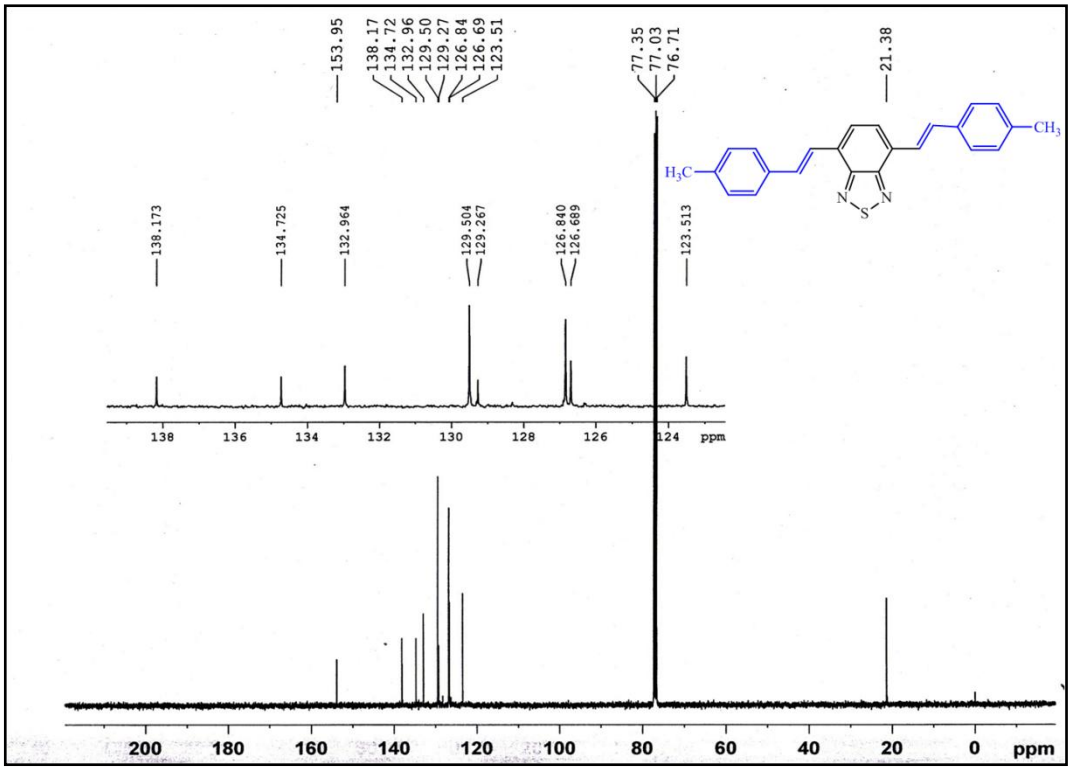

^{13}C-NMR of Compound **21**

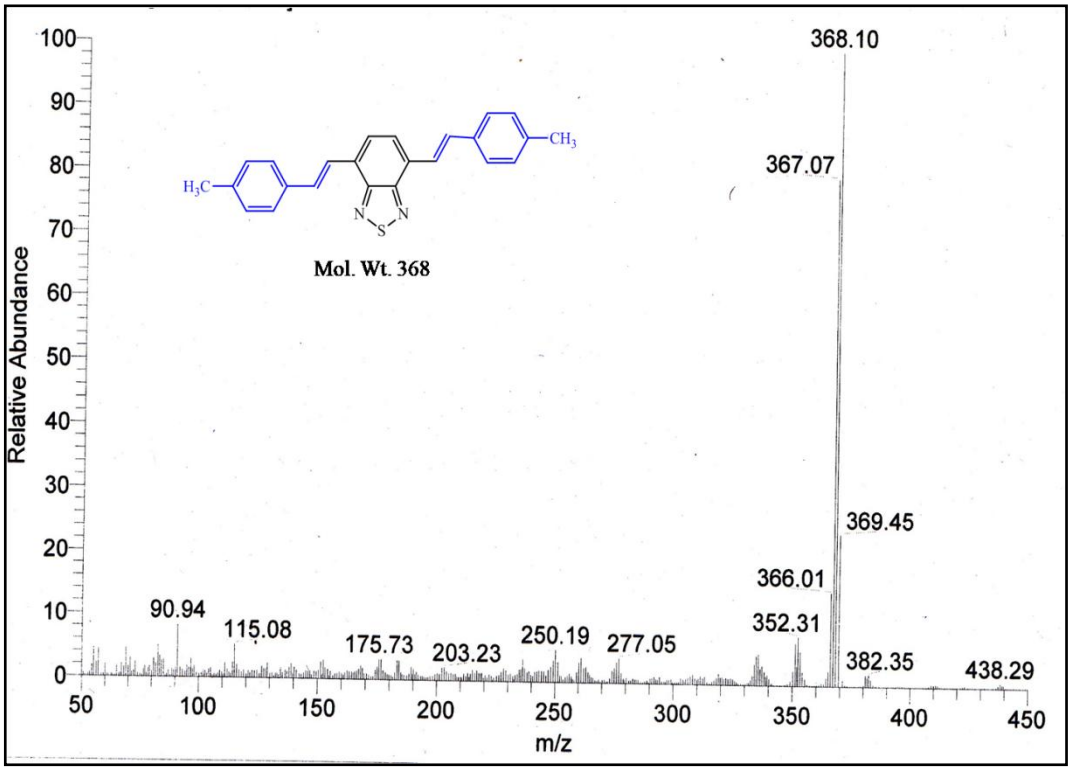

Mass Spectra of Compound **21**

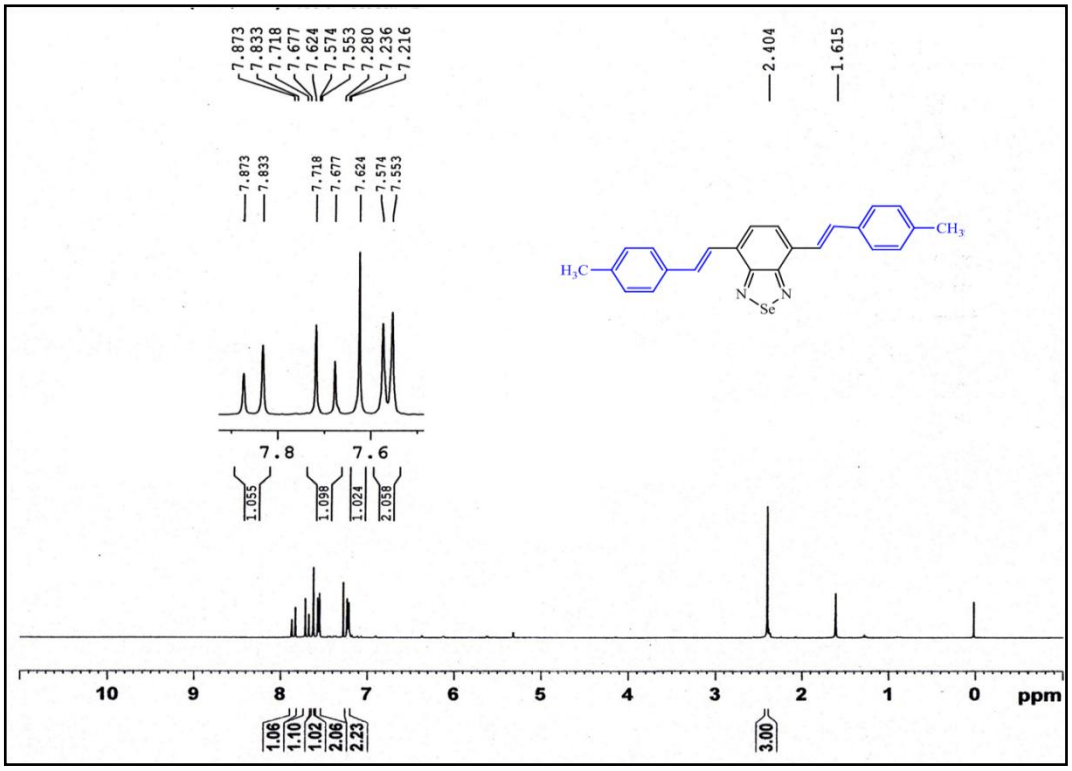

^{1}H-NMR of Compound **22**

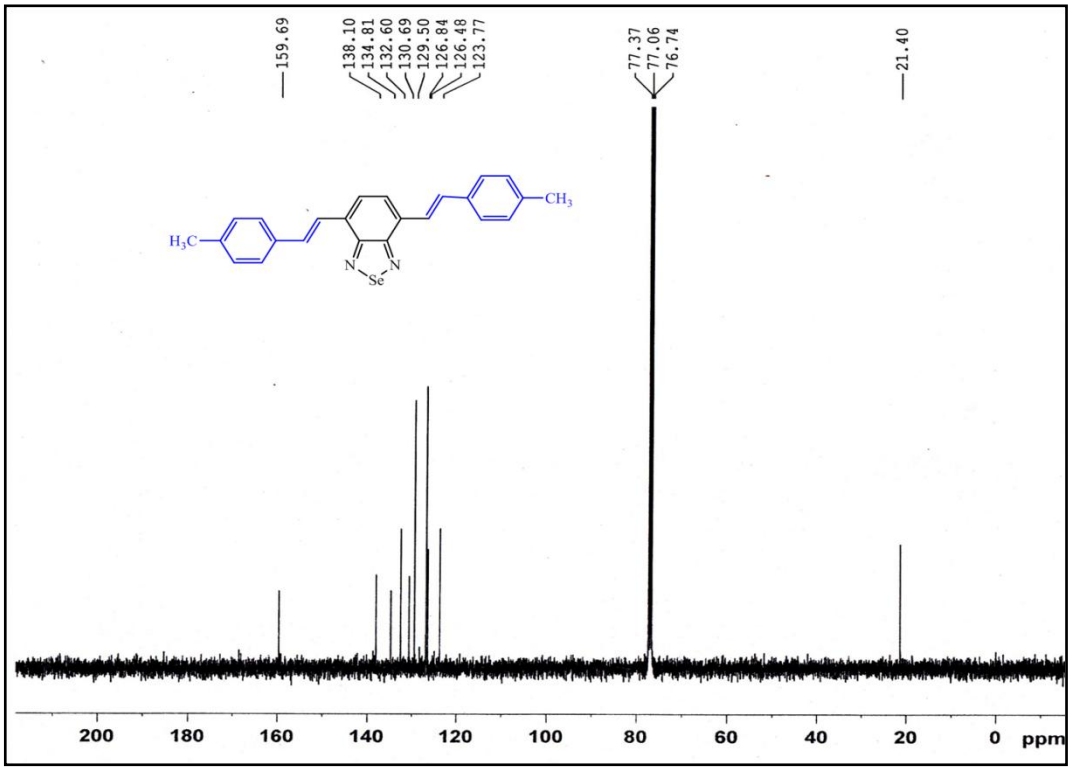

^{13}C-NMR of Compound **22**

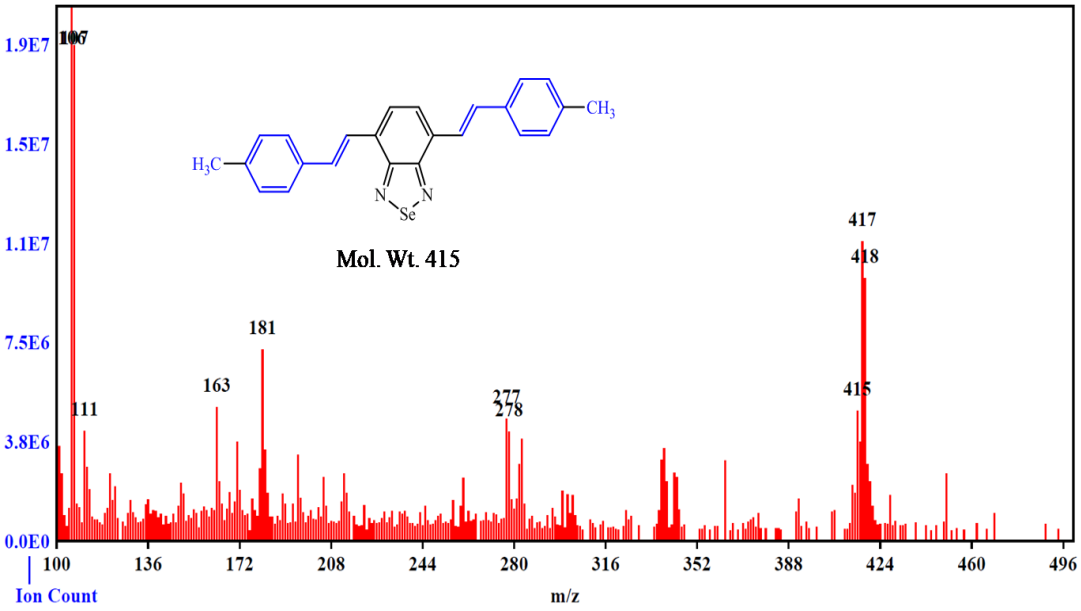

Mass Spectra of Compound **22**

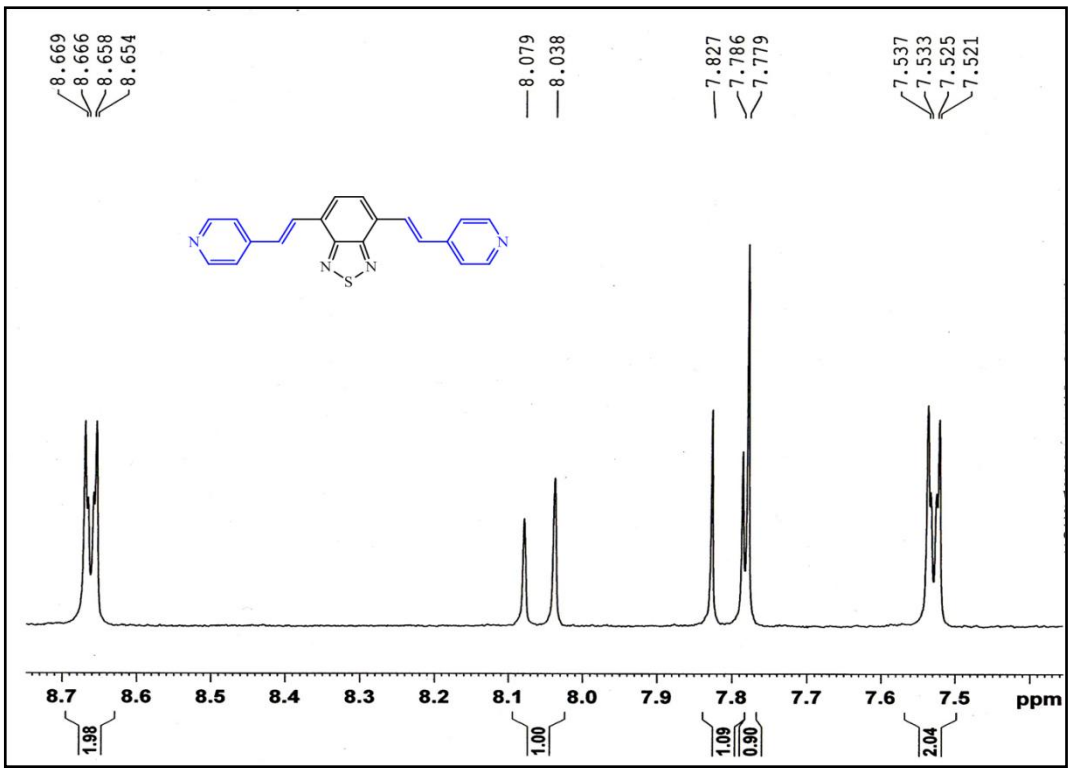

^{1}H-NMR of Compound **23**

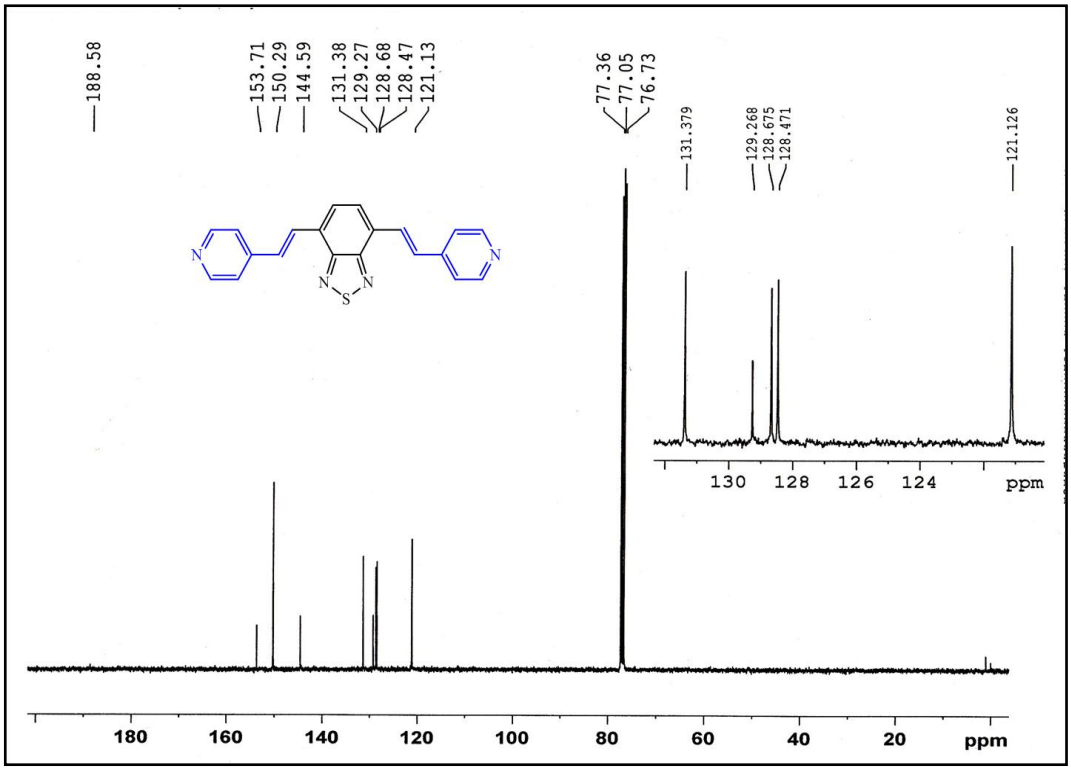

^{13}C-NMR of Compound **23**

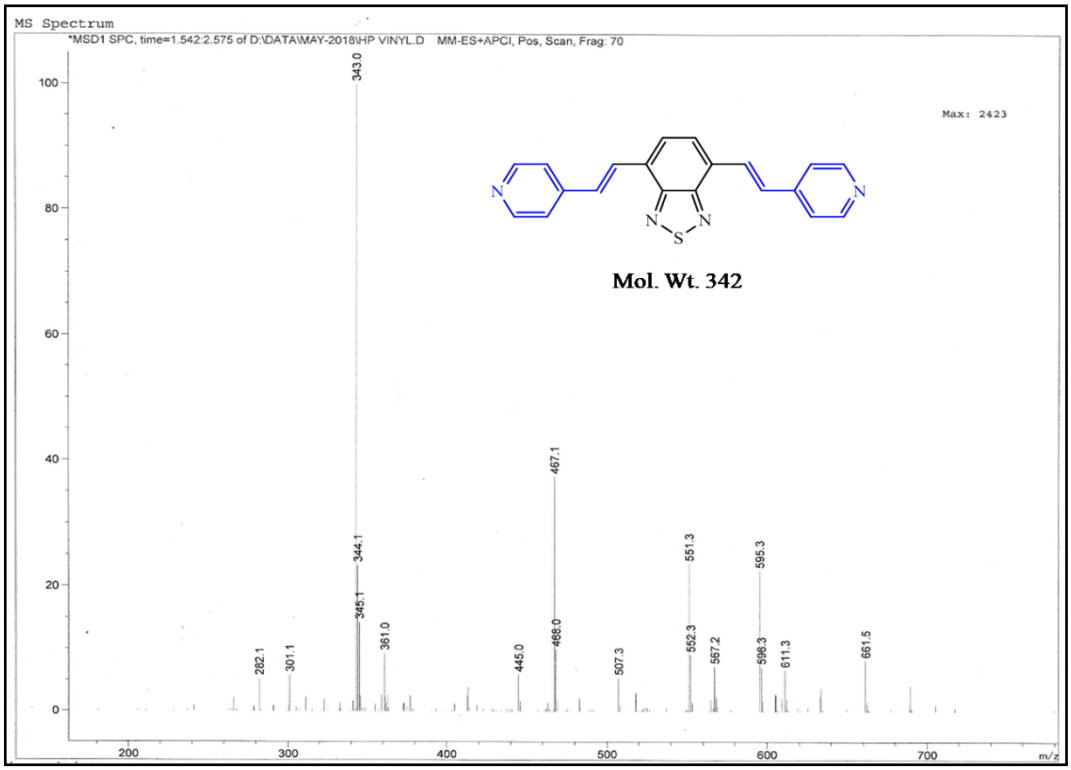

Mass Spectra of Compound **23**

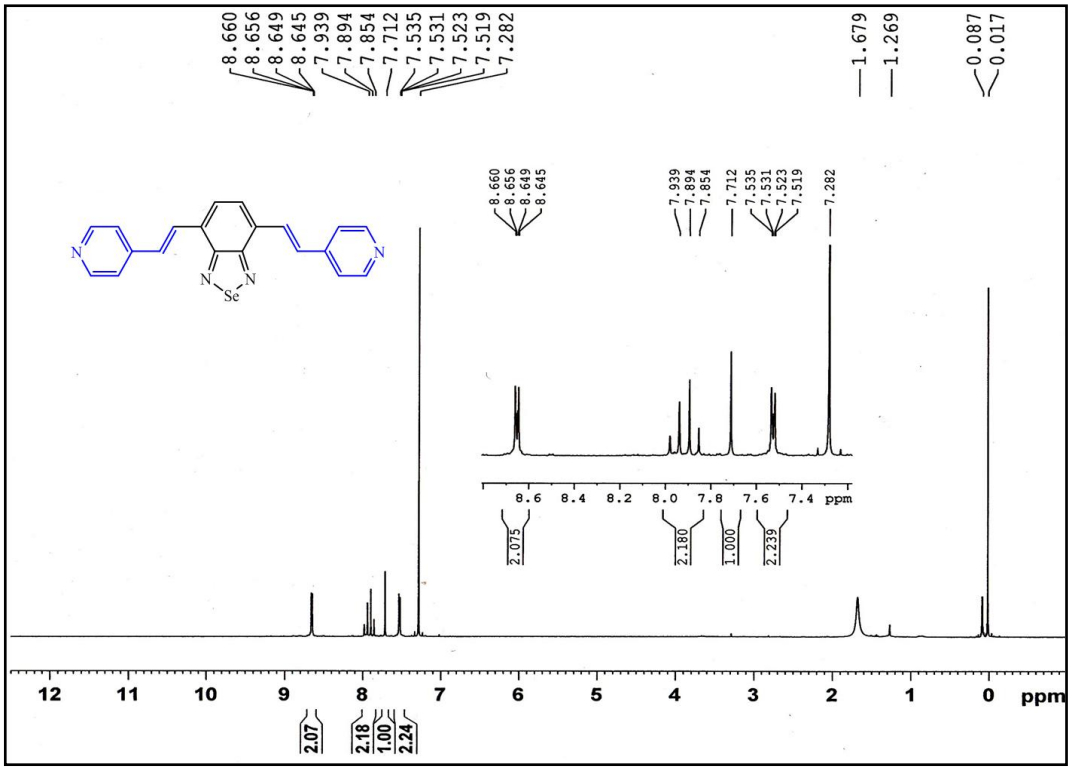

^{1}H-NMR of Compound **24**

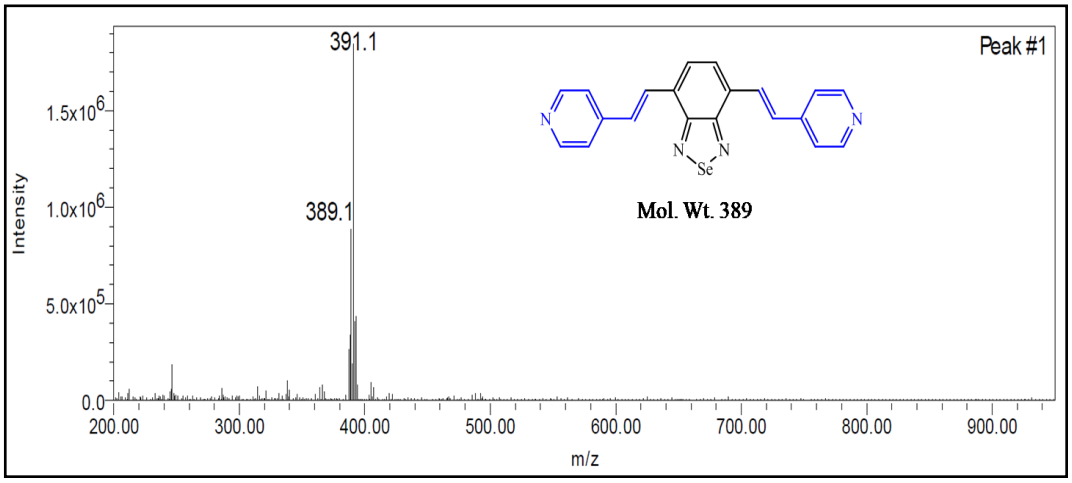

Mass Spectra of Compound **24**

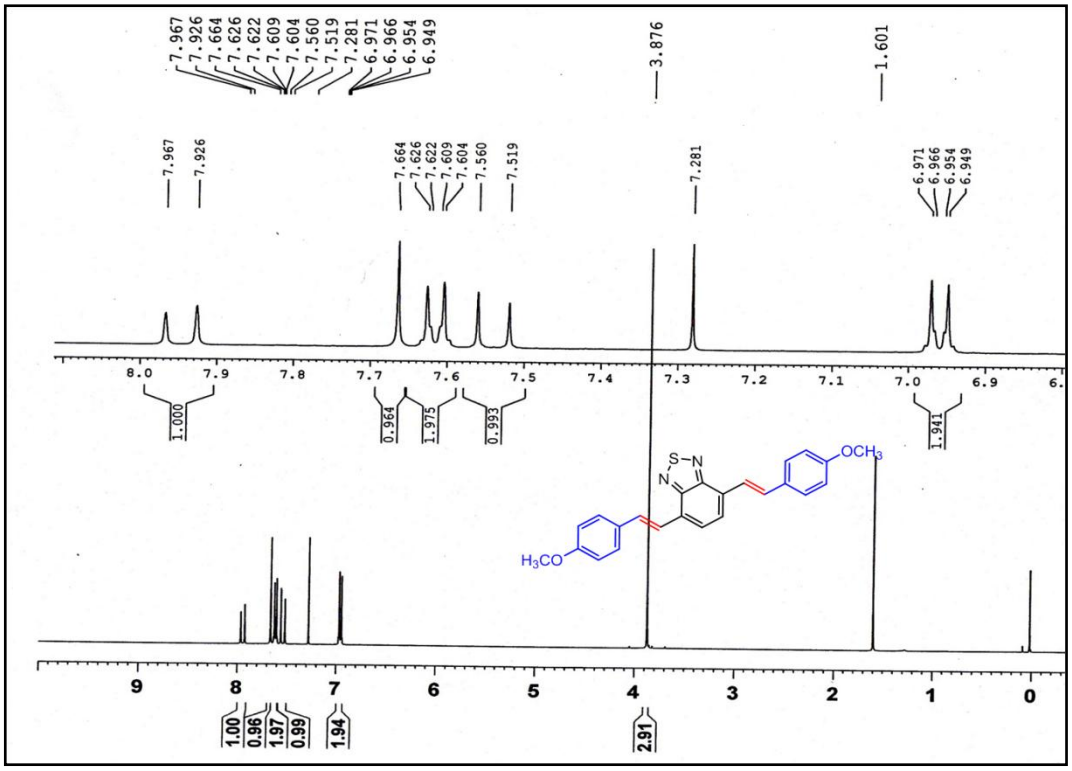

^{1}H-NMR of Compound **25**

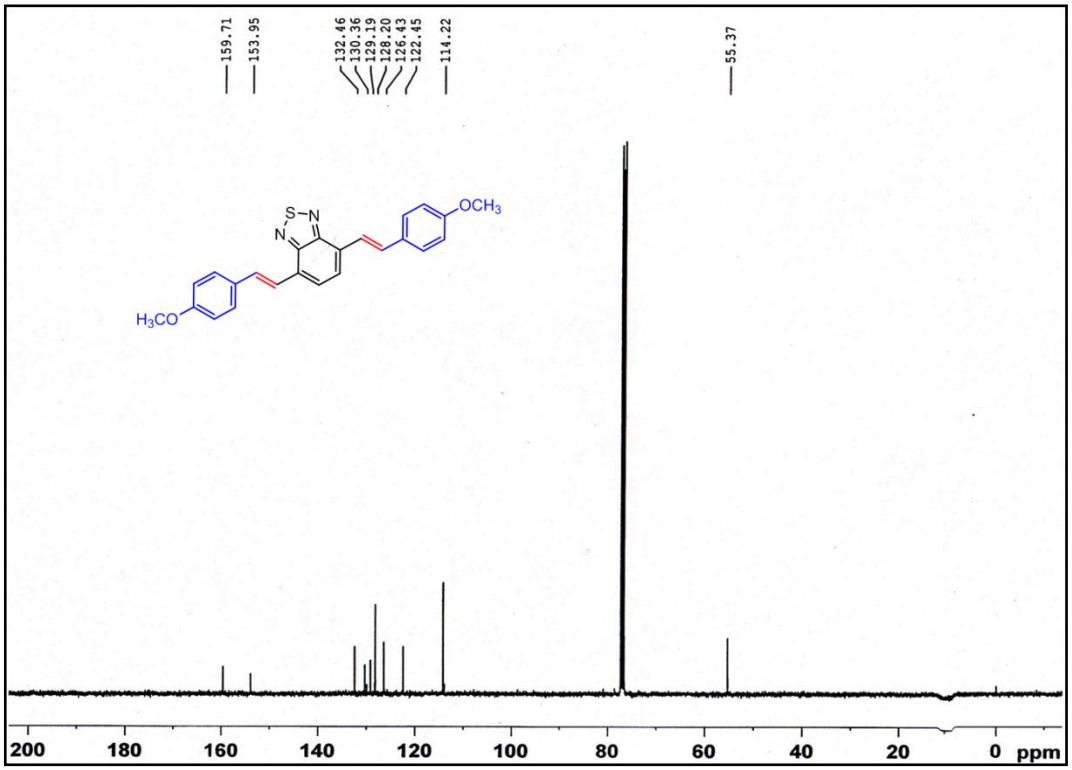

^{13}C-NMR of Compound **25**

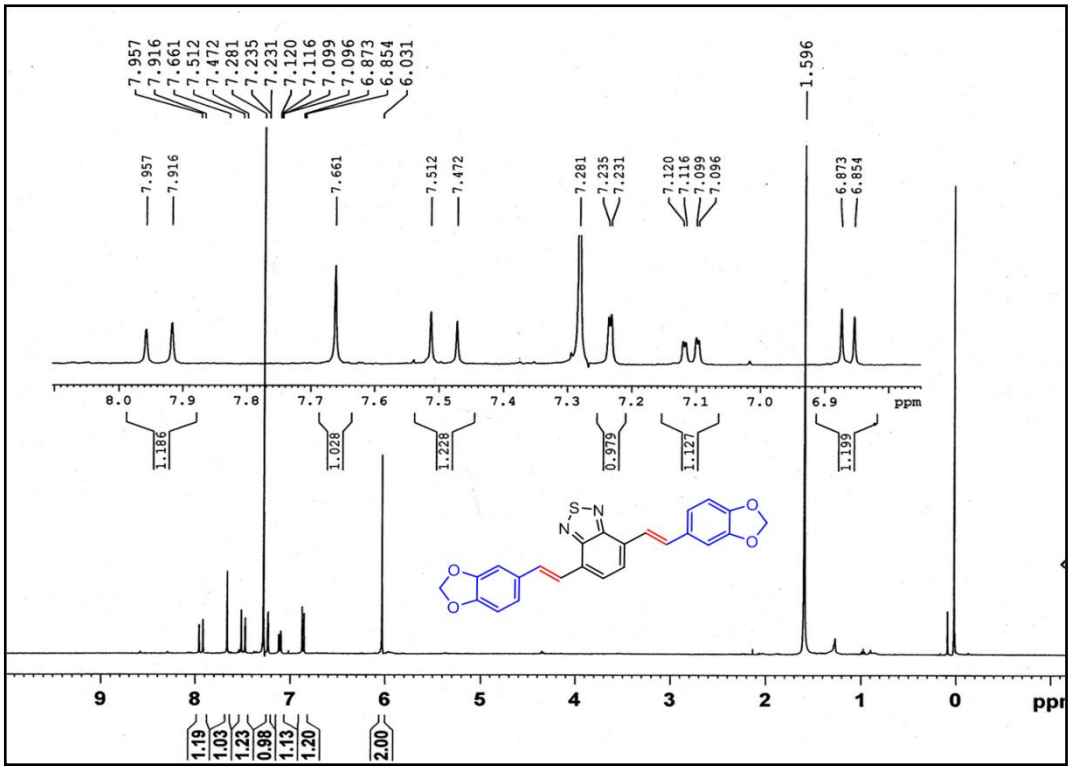

^{1}H-NMR of Compound **26**

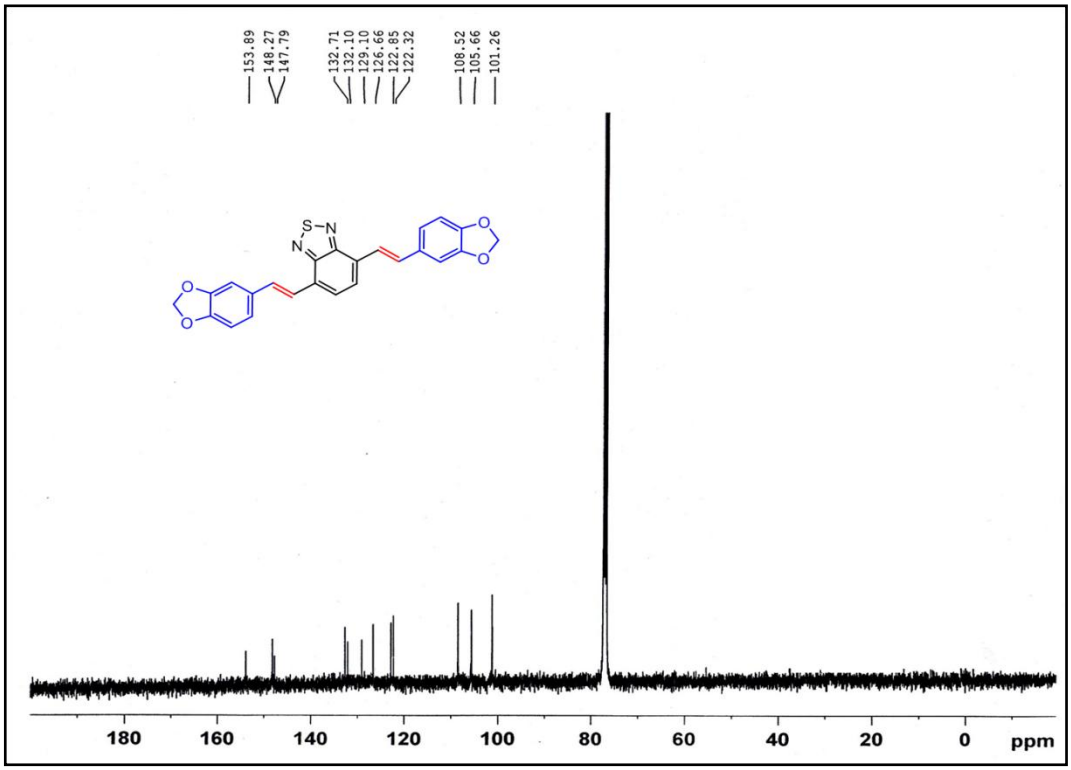

^{13}C-NMR of Compound **26**

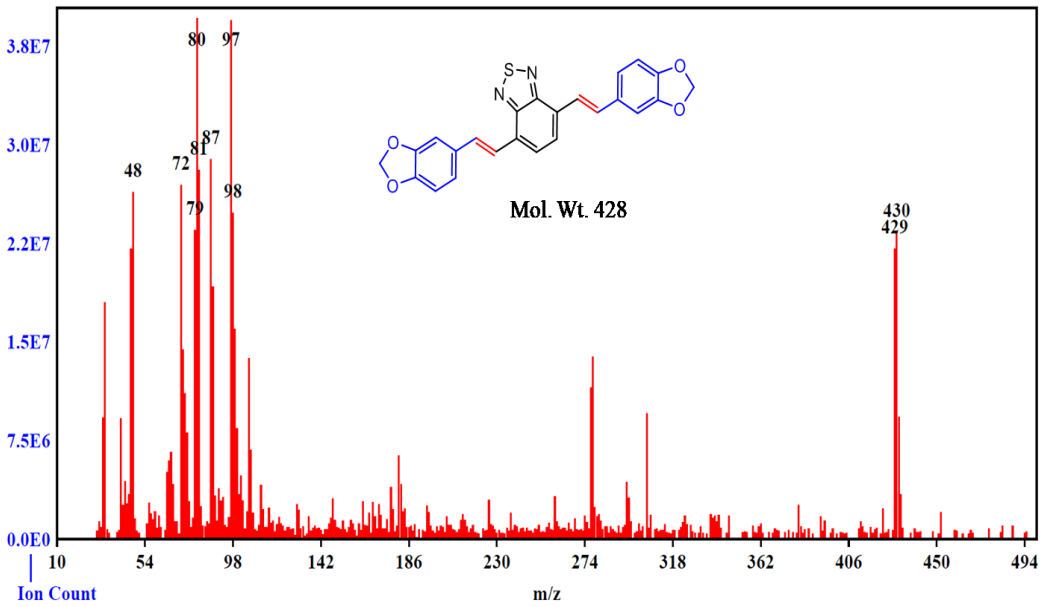

Mass Spectra of Compound **26**

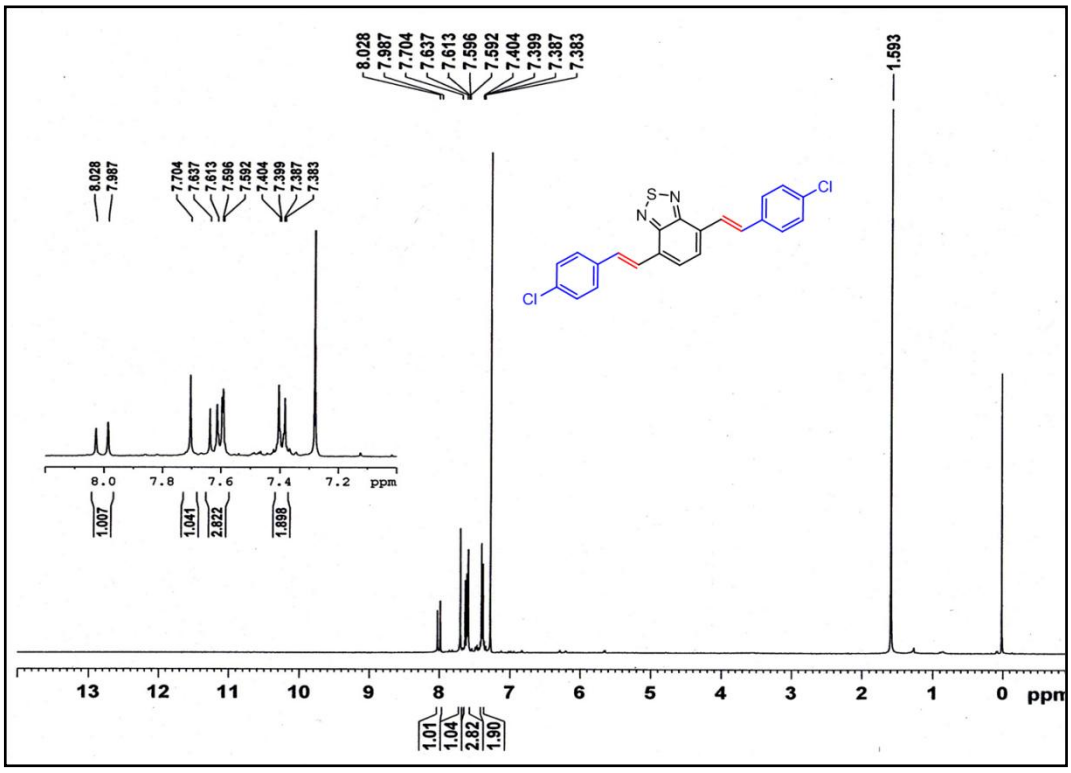

^{1}H-NMR of Compound **29**

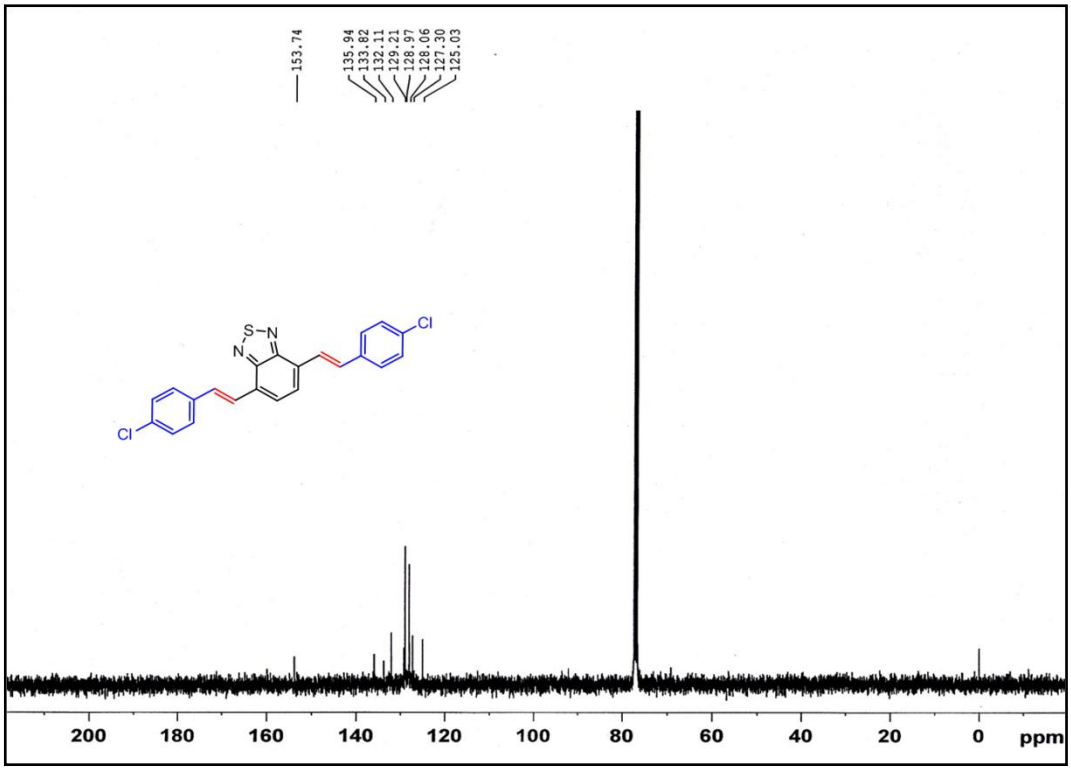

^{13}C-NMR of Compound **29**

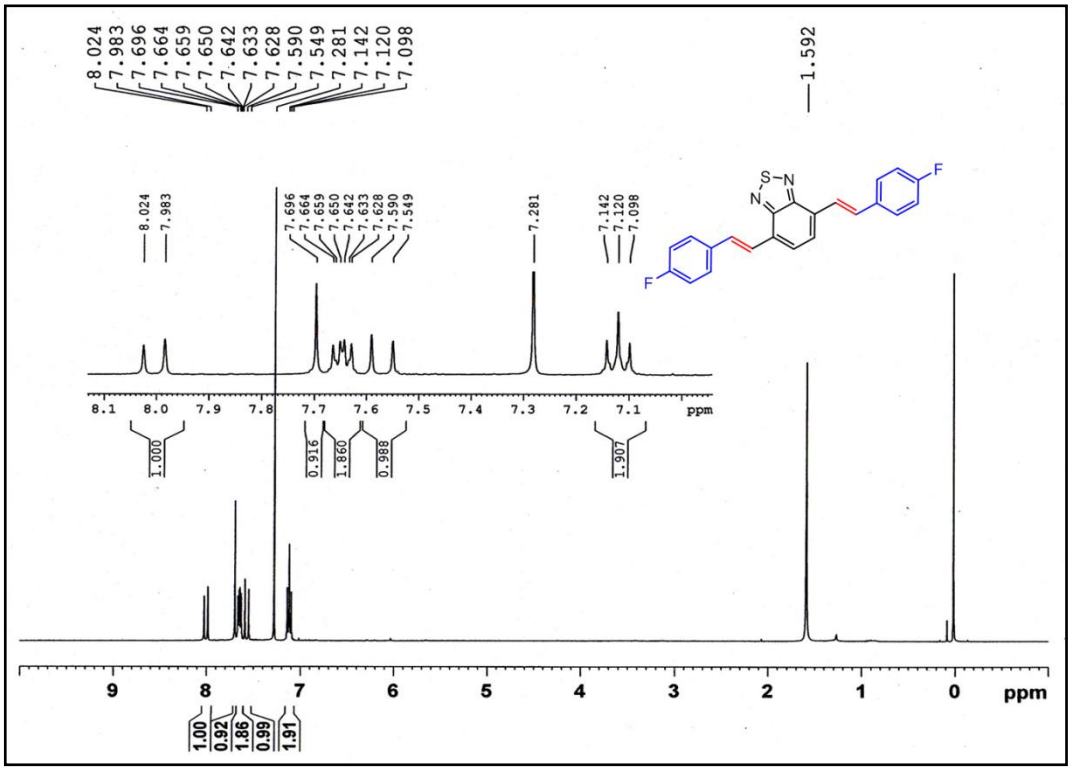

^{1}H-NMR of Compound **30**

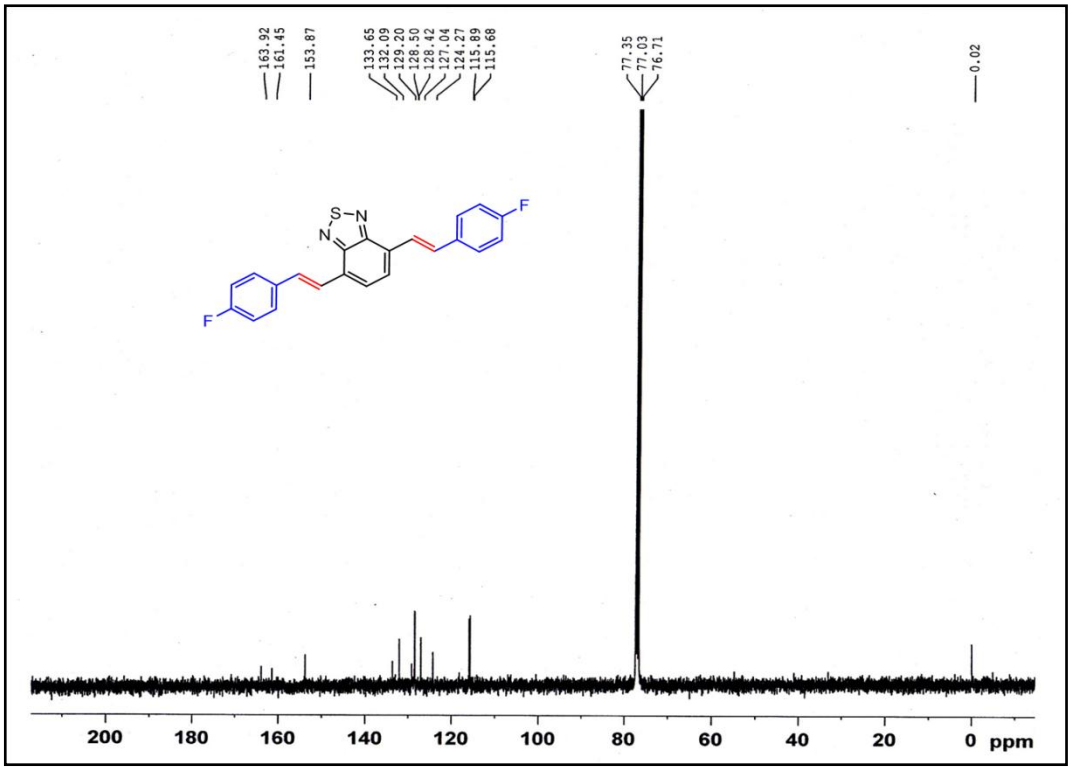

^{13}C-NMR of Compound **30**

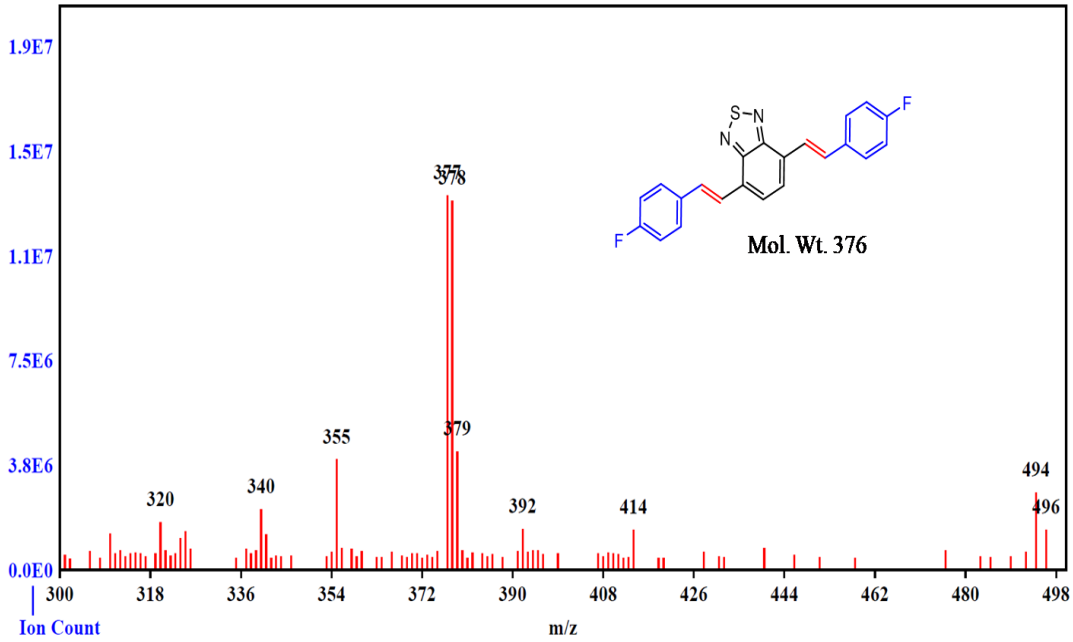

Mass Spectra of Compound **30**

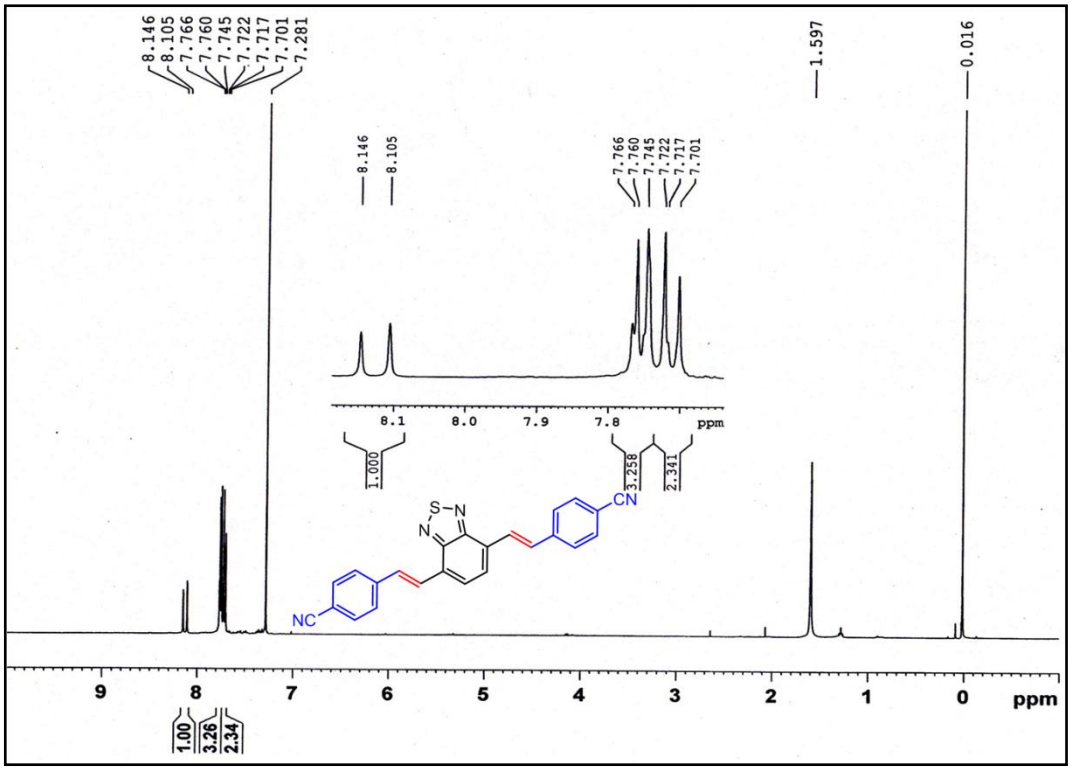

^{1}H-NMR of Compound **31**

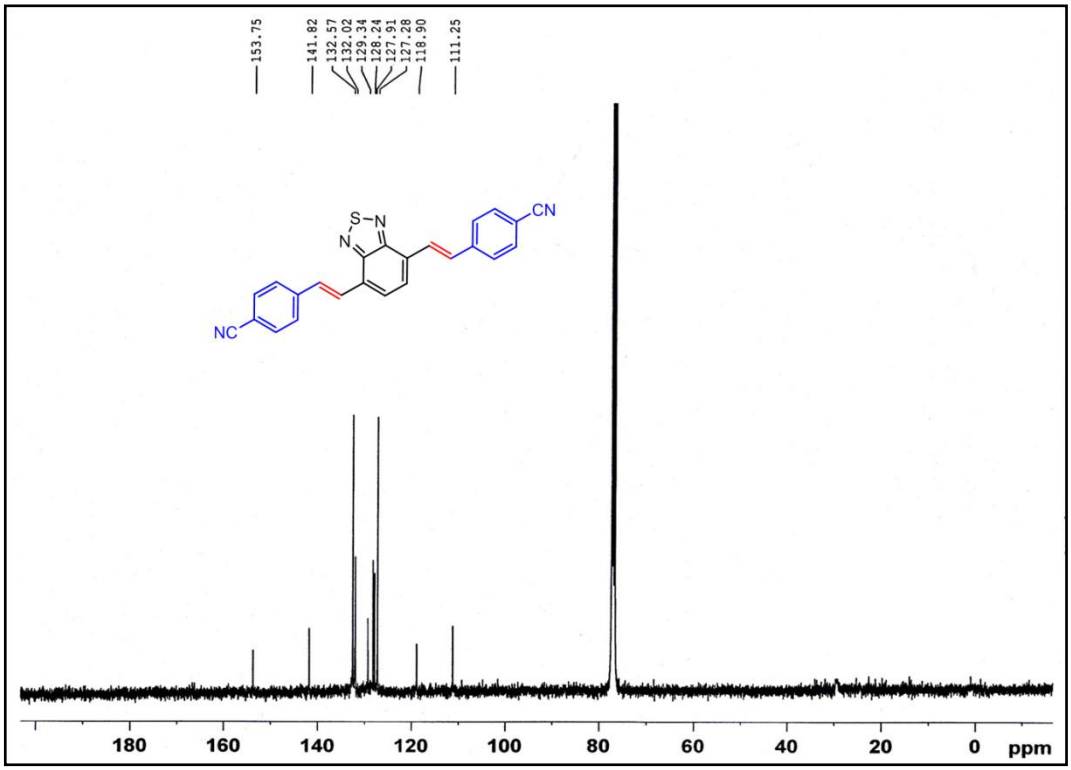

^{13}C-NMR of Compound **31**

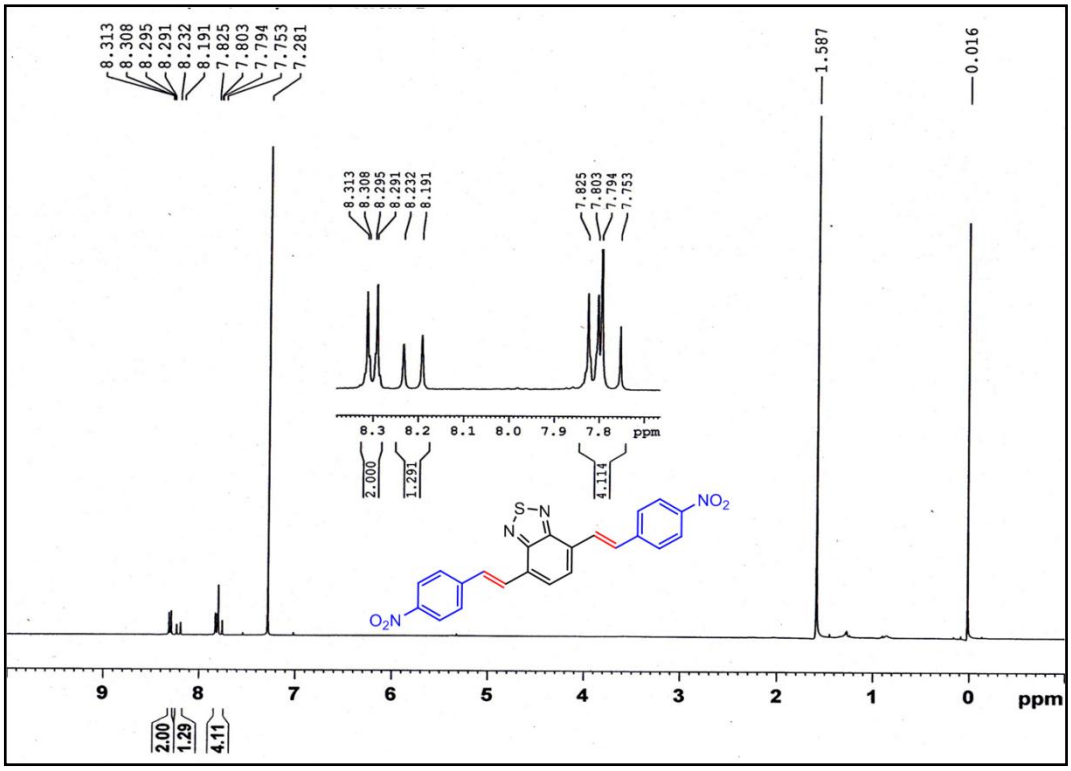

^{1}H-NMR of Compound **32**

4.5 References

1. E.E. Havinga, W. Ten-Hoeve, H. Wynberg, *Polym. Bull.* **1992**, *29*, 119.
2. P.B. Pati, S.S. Zade, *Cryst. Growth Des.* **2014**, *14*, 1695.
3. I.F. Perepichka, D.F. Perepichka, Handbook of Thiophene-Based Materials: Applications in Organic Electronics and Photonics; Wiley: New York, 2009.
4. Z. Lin, J. Bjorgaard, A.G. Yavuz, M.E. Kose, *J. Phys. Chem. C* **2011**, *115*, 15097.
5. P.B. Pati, S.P. Senanayak, K.S. Narayan, S.S. Zade, *ACS Appl. Mater. Interfaces* **2013**, *5*, 12460.
6. J.J. Bryant, B.D. Lindner, U.H.F. Bunz, *J. Org. Chem.* **2013**, *78*, 1038.
7. T. Ishi-i, M.Sakai, C. Shinoda *Tetrahedron* **2013**, *69*, 9475.
8. M.N.K.P. Bolisetty, C.-T. Li, K.R.J. Thomas, G.B. Bodedla, K.-C. Ho, *Tetrahedron* **2015,** *71*, 4203.
9. (a) M. Dietrich, J. Heinze, G. Heywang, F. *J. Electroanal. Chem.* **1994**, *369*, 87. (b) A. Patra, Y.H. Wijsboom, S.S. Zade, M. Li, Y. Sheynin, G. Leitus, M. Bendikov, *J. Am. Chem. Soc.* **2008**, *130*, 6734.
10. D.Wen, Y.Y. Fu, L.Q. Shi, C. He, L.Dong, D.F. Zhu, Q.G. He, H.M.Cao, J.G.Cheng, *Sensors and Actuators B*, **2012**, *168*, 283.

11. S. Xu, Y. Liu, J. Li, Y. Wang, S. Cao, *Polym. Adv. Technol*. **2010**, 21, 663.
12. K.N. Patel, A.V. Bedekar *Tetrahedron Lett.* 2015, *56*, 6617.
13. Z. Liu, J. He, H. Zhuang, H. Li, N. Li, D. Chen, Q. Xu, J. Lu, K. Zhanga, L. Wang, *J. Mater. Chem. C*, **2015**, *3*, 9145.
14. (a) S. Das, P.B. Pati, S.S. Zade, *Macromolecules* **2008**, *45*, 5410. (b) G.L. Gibson, T.M. McCormick, D.S. Seferos, *J. Am. Chem. Soc.* **2012**, *134*, 539.
15. (a) Y. Park,C-Y. Kuo, J.S. Martinez, Y.S. Park, O. Postupna, A. Zhugayevych, S. Kim, J. Park, S. Tretiak, H-L. Wang, *Appl. Mater. Interfaces* **2013**, *5*, 4685. (b) A.J. Zucchero, J.N. Wilson, U.H.F. Bunz, *J. Am. Chem. Soc***. 2006**, *128*, 11872.
16. G.R. Desiraju, Cryst. Eng., The Design of Organic Solids, Elsevier, Amsterdam, 1989.
17. R. Ganduri, S. Cherukuvada, S. Sarkar, T.N.G. Row**,** *Cryst. Eng. Comm.* **2017**, *19*, 1123.
18. B.R. Bhogala, S. Basavoju, A. Nangia *Cryst. Eng. Comm.* **2005**, *7*, 551.
19. (a) C.B. Aakeroy, J. Desper, J.F. Urbina, *Chem. Commun*. **2005**, 2820. (b) Y.-H. Luo, B.-W. Sun, *Spectrochim. Acta A* **2014**, *120*, 228.
20. A.S. Saiyed, A.V. Bedekar, *Tetrahedron Lett.* **2010**, *51*, 6227.
21. I. Idris, F. Derridj, J.-F. Soule, H. Douceta, *Adv. Synth. Catal.* **2017**, *359*, 2448.
22. F.S. Mancilha, B.A.D Neto, A.S. Lopes, P.F. Moreira Jr., F.H. Quina, R.S. Goncalves, J. Dupont, *Eur. J. Org. Chem.* **2006**, 4924.
23. P.B. Pati, S. Das, S.S. Zade, *J. Polym. Sci., Part A: Polym. Chem.* **2012**, *50*, 3996.
24. S. Mattiello, M. Rooney, A. Sanzone, P. Brazzo, M. Sassi, L. Beverina, *Org. Lett.* **2017**, *3*, 654.